Dynamical Climatology

Observing System experiments using the Meteorological Office's 15-Level model.

by

R.A. Bromley

DCTN 16 January 1985

Meteorological Office (Met. O. 20)
London Road
Bracknell
Berkshire RG12 2SZ

DYNAMICAL CLIMATOLOGY TECHNICAL NOTE NO. 16

OBSERVING SYSTEM EXPERIMENTS USING THE METEOROLOGICAL OFFICE'S 15-LEVEL MODEL

by

R.A. Bromley

This paper has been submitted for publication in the Proceedings of the 1984 ECMWF Seminar/Workshop on Data Assimilation Syatems and Observing System Experiments with Particular Emphasis on FGGE.

Met O 20 (Dynamical
Climatology Branch)
Meteorological Office
London Road
Bracknell
Berkshire, U.K. RG12 2SZ

January 1985

OBSERVING SYSTEM EXPERIMENTS USING THE METEOROLOGICAL OFFICE'S 15-LEVEL MODEL

R.A.Bromley

Meteorological Office, Bracknell, UK

1. INTRODUCTION

Thanks to the extra observing devices deployed, the global observing system during FGGE produced the greatest cover of meteorological data over the whole global atmosphere that is currently available. Some of the extra observing systems have since ceased to operate, but most of the FGGE systems, or their replacements, are still returning observations. It is therefore relevant to enquire what effect the different types of observation may have on numerical models of the atmosphere. The impact of a set of observations is not easily defined since the various types report different fields and each set is distributed in a different way over the surface of the Earth. An empirical approach has to be adopted in order to study the impact of each system: where two comparable model states are produced from different sets of observations, the changes observed from one state to the other are due to the differences between the observation sets. The impact is the complete set of changes so induced. These changes may be qualitative, as we shall see in the examination of several versions of the same synoptic situation, but they can also be expressed in various quantitative forms. The impact may be found on a number of scales of space or time: it may be local, regional or global; and it may occur immediately the observations are assimilated or it may build up over a period of model time.

The design of the model also has a significant role in determining the way that observations are allowed to affect the model state (Hollingsworth et al, 1983) and so, where possible, it is desirable to conduct impact studies in parallel on more than one numerical model. The studies reported below deal with the same case as is treated elsewhere at this seminar by workers from ECMWF (Tibaldi, 1984) and the Japanese Meteorological Agency (Kashawagi, 1984).

2. THE NUMERICAL MODEL

The studies reported here have been carried out using the 15-level operational forecasting system of the UK Meteorological Office. This system has been described in detail elsewhere (Bell (1983), Foreman (1983)), but some important features are discussed below. Since the system has been designed for operational forecasting, it has been tuned according to criteria obtained mainly from the performance of the model forecasts. Such a system does not necessarily produce an analysis to fit the data as closely as possible. Hence the impact of additional data must be investigated in forecasts as well as in analyses.

The forecasting system works in the stages illustrated in Figure 1. The basic cycle of the model for data time T starts from the analysis for T-6: it also uses a forecast from this analysis as the first-guess field for time T. Having assimilated data from T-6 to T, to produce the analysis at T, the model is run forward a further 6 hours to generate the background forecast for the next cycle.

The system includes stages for the extraction and pre-processing of the observations in preparation for assimilation into the model. During these stages, multi-level data (ie reports containing observations at several levels in the vertical, for example radiosonde reports) are

transferred from the pressure levels on which the observations were made on to the sigma levels of the model. A single-level report, however, is held on the original pressure level until it is assimilated, when it is allowed to affect at least the nearest two sigma levels, one above and one below. Assimilation is carried out by repeated insertion of the observational increments using weights appropriate to optimum interpolation.

The following features of the data assimilation scheme should also be noted.

1. Geostrophic wind increments are used to help the assimilation of temperature information not otherwise supported by wind data. This is done to counteract the tendency for wind information to be assimilated faster than mass information in typical synoptic-scale weather systems.

2. Hydrostatic increments of potential temperature are applied in the vertical column above an observation of surface pressure. This prevents changes in the surface pressure field from causing excessive changes in the height field at upper levels.

3. Divergence diffusion is applied in order to reduce the amplitudes of the gravity waves that are set up whenever an observation is assimilated.

These features will be seen to have had an effect on the impact studies reported below.

3. PROCEDURE

The overall scheme for running several studies for the same case is illustrated in Figure 2.

A case was chosen from Special Observing Period 1 of the FGGE year to ensure the maximium cover of observations. A winter case with significant developments over the North Atlantic was chosen because of

the importance of this area to weather forecasting over Europe but there were notable developments in several other parts of the globe. During SOP-1 the circulation was slow-moving over the North Atlantic so that the most worthwhile case was found near the end of the period, starting on 27th February.

The experiments were begun from the Level III-B analysis for Day-4 (23rd February), obtained from ECMWF. This analysis was transformed to the horizontal and vertical grid of the 15-level model and was subjected to the assimilation of all available data for two model days, from Day-4 to Day-2, to allow the model to adjust to a state determined by the tuning of the 15-level system. In a similar experiment, Barwell and Lorenc (to be published, 1985) found that two model days is sufficient time for the model atmosphere to adjust from one numerical system to another.

The observations for assimilation were copied from the Level II-B data held at ECMWF. Charts of the distribution of satellite observations are given in Figures 3a, b. Charts showing the distribution of other observation types may be found in Bjorheim et al (1981). Control assimilations using all the II-B data continued from Day-2, through Day 0, to Day 6. A control forecast was then obtained by running a forecast to Day 6, starting from the control analysis for Day 0. To observe the impact of a chosen sub-system of the full global observing system, a further assimilation was performed over the period Day-2 to Day 0 with the observations in question entirely absent from the assimilated data. The analysis at Day 0, as produced by the depleted set of observations,

was then used as the starting point for a forecast run to Day 6. A summary of the components of the various observing systems used in this study is given in Table 1.

Once the assimilations and forecasts had been completed the studies turned to the identification and explanation of the differences between the control runs and the depleted assimilations and forecasts from them. This was done mainly by comparing different treatments of the same synoptic features but rms differences and an expression for the correlation of the differences were also considered.

4. THE IMPACT STUDIES

4.1 Experiments IA0 and IA1: The Control Assimilation and Forecast

These model runs used all the available Level II-B observations up to Day 0. The control assimilation continued to use all available data to produce analyses every 6 hours up to Day 6. The control forecast was a normal forecast starting from the control analysis for Day 0 and running as far as Day 6. The analyses and forecasts are shown in chronological order in Figure 4. There is general agreement between the IA0 analyses and the Level III-B analyses published by ECMWF (Bjorheim et al, 1981), apart from some minor discrepancies.

The control analyses show that at Day 0 there was a belt of high pressure from Canada to the Black Sea (Fig 4a). To the north of this belt an old depression near Spitzbergen was filling but there was another depression near the Denmark Strait with troughs on its southern side, one extending towards Iceland and one towards Labrador. To the south of the belt were two further depressions, one over the Eastern seaboard of the USA and one near (30 N, 45 W). As the atmosphere developed through the period of the case study (Fig 4a, c, g, k), the high-pressure belt

resolved itself into an anticyclone initially over the Eastern Atlantic, but moving very slowly towards the Iberian peninsula and maintaining its intensity throughout. Meanwhile the main depression near Iceland swung northwards and the lows originally to the south progressed around the anticyclone to appear as secondary features in a trough extending southwestwards from the main low-pressure complex by Day 3. A strong westerly flow, initially to the south of Iceland, was gradually extended over North-West Europe, carrying the trough over Iceland at Day 0 to about 60 E by Day 6, after disrupting between Days 2 and 3 to leave a low-pressure area over the Western Mediterranean.

The Southern Hemisphere (Figures 4b, e, i, m) was much more zonal than the Northern, with a train of depressions proceeding slowly westwards through a belt of latitude bounded by Antarctica to the south and the mid-latitude anticyclones over each ocean to the north. Three of the low-pressure areas will be considered in the later experiments. The first of these is the depression over Cape Horn on Day 0 which deepened, slowly at first and then rapidly, to be an intense feature at (60 S, 30 W) on Day 3: the second is the rather ill-defined feature initially to the south of South Africa which moved steadily eastwards to reach 90 E by Day 3: and the third is the semi-permanent area of low-pressure over Australia from where occasional troughs extended southwards towards the Southern Ocean and Tasmania.

The control forecast, IA1, has treated developments over the Northern Hemisphere quite well (Figs 4d, h, l), with some loss of detail but with all the major features in place. Although the Icelandic low was not forecast deep enough and the secondary centres were sometimes poorly defined, the troughs that moved around this low were well forecast

as far as Day 3. The evolution of the low over the Western Mediterranean was predicted but it was 10 degrees too far East on Day 3. Even at Day 6, the general character of the pressure field was forecast satisfactorily, despite some errors in the prediction of the Icelandic complex and of the situation over the Mediterranean.

Over the Southern Hemisphere the control forecast was less successful (Figs 4f, j, n). The low over the South Atlantic showed serious errors early on and the deepening on Day 3 was not predicted. By this stage of the forecast there were several serious errors, but the low near 90 E and the situation over the Eastern Pacific were reasonably correct.

4.2 Experiment IA2: SATEMs omitted

All observations except SATEMs were used in the assimilation over the 48-hour period up to Day 0. A forecast to Day 6 was then run from the analysis for Day 0. A general study of the difference between this forecast and the control runs showed that the greatest impact was at 250 mb and so the discussion will concentrate on this level. Two areas were selected for detailed examination.

4.2.1 North Atlantic Case

The depression over mid-Atlantic is one component of the familiar omega-shaped blocking pattern. It therefore has an important role in the circulation and it must be treated accurately if a forecast is to be acceptable. However, without SATEMs present this feature has been analysed up to 6 dam weaker at 250 mb (Fig 5a). The wind perturbation field on the north side of the system is clearly ageostrophic. After 24 hours of the forecast, however, (Fig 5b) the ageostrophy has disappeared and the height difference between the fields has been reduced, not only

at 250 mb, but at all levels examined. Once it is balanced, the difference pattern shows its maximum slightly to the south of the centre of the low and it maintains this relative position as the system is carried around the anticyclone. During Days 2 and 3 (Figs 5c, d) the height difference increases again but the wind difference increases correspondingly, thus maintaining the geostrophic balance between these fields. Overall it appears that most of the balanced part of the difference is retained. This would have a beneficial effect in the control forecast IA1.

4.2.2 Southern Hemisphere

The large differences at 250 mb at analysis time (Fig 6a) indicate that the SATEMs had a considerable impact in the Southern hemisphere. Perhaps because of the scarcity of other observations, the difference fields at Day 0 appear to be better balanced than in the North Atlantic case just discussed. As the forecast progresses the nature of the impact becomes clearer. In many parts of the Southern Hemisphere the development of the initial difference field is such that by Day 3 the forecast from the analysis without SATEMs was clearly more successful than the forecast from the analysis including SATEMs (Fig 6b): in particular the deep low near (60 S, 15 W) was predicted much better and the depressions near (50 S, 90 E) and (60 S, 170 W) were also improved.

The distribution of SATEM observations for 00Z on 27th February (Day 0)is shown in Figure 3a. In the vicinity of South America south of 45 S there were many SATEMs available but the majority are in the TIROS-N swathes to the west of 60 W. The difference patterns associated with the erroneous South Atlantic low can be traced back to Tierra del Fuego on Day 0, just within the area of TIROS-N coverage. Although the starting

analyses in this area show no significant differences in pmsl, it is apparent from Figures 6c and d that IA2 has a different thickness pattern from IAO at Day 0. This implies a difference in thermal structure at or below 500 mb. The inclusion of the SATEM data in IAO thus appears to have produced an error in the thermal structure, which has prevented the correct prediction of the subsequent behaviour of the low in IA1. Whether the fault is caused directly by bad data or by the model's mishandling of the data, is not yet clear.

It should be noted that although this discussion has highlighted a significant fault, there are other areas in the Southern hemisphere which are improved when the SATEMs are included. The total effect of adding the SATEMs is a set of large changes, both beneficial and detrimental, distributed over the whole hemisphere: taken together, these changes result in a beneficial impact overall.

4.3 Experiment IA3: SATOBs omitted

All observations except SATOBs were used in the assimilation from Day-2 to Day 0 and the resulting analysis was the starting state for a forecast run to Day 6.

Because SATOBs are distributed between 50 N and 50 S, their impact on the analysis is limited to about these latitudes, as shown by the zonal cross-section of vector wind-differences (Fig. 7a). At about 250 mb the main features of the cross-section are found around the sub-tropical jet in the Northern Hemisphere, over the Equator, and, rather more weakly, over the broad band of strong upper winds in the Southern Hemisphere. In the Northern Hemisphere the sub-tropical jet is analysed much stronger when SATOBs are incuded, whereas over the Equator

(where the geostrophic relationship is of no assistance), the SATOBs have a similar impact in a much lighter flow simply because they comprise the majority of wind observations available.

By Day 3 of the forecast the difference pattern has spread out towards the poles (Fig 7b). It also appears that by this time the features seen at about 700 mb in the analysis have disappeared, but cross-sections of the intervening forecasts suggest that the difference moves upwards with time. If this is so, then the maximum at 700 mb may be due to the vertical propagation of SATOB information assimilated at an early stage in the period from Day-2 to Day 0.

4.3.1 North Atlantic case

It is fortunate that the depression over mid-Atlantic is conveniently placed for the assessment of the impact of both SATEMs and SATOBs. In the area of this depression, the set of SATOBs at analysis time was mostly made up of low-level winds to the south of 30 N but there were a few high-level observations to the east of the surface centre. (There is very little tilt of the axis with height). The difference field at Day 0 (Fig 8a) is obviously due to the accumulated effect of the SATOBs and not just those for 00Z on Day 0. The pattern is a good example of a typical correction to the wind - at about (35 N, 40 W) -with a supporting perturbation in the height field. The difference fields due to SATOBs were in a better geostrophic balance at Day 0 than was the case for SATEMs but the height difference tends to be negative. During the forecast the SATOB perturbation behaves like the SATEM perturbation, first weakening on Day 1, but then strengthening again on Day 2 as it is carried around the low and into the main jet (Figs 8b, c, d). By Day 3

however the SATOB perturbation has almost dissipated and all that remains is a small correction to the flow pattern and a negligible change to the heights.

4.3.2 The Tropical Atlantic

This case was chosen in order to examine analyses in a reasonably large sector of the tropics, where SATOBs are the main source of wind information. The low-level wind flow over the tropics is important in a number of phenomena so a comparison has been made of the 850 mb wind analyses both with SATOB included (IA0) and with SATOBs omitted (IA3).

The divergent (irrotational) and non-divergent components of the analysed winds are shown in Figure 9a, b, c, d. It is apparent that the divergence damping has had the desired effect, making the divergent part of the wind much the weaker component. The only area of difference between the analyses of the divergent wind is north of 15°N, on the southern edge of the Atlantic depression already discussed. Differences over this area can also be seen in the non-divergent component, where the position of the strongest flow seems to be more realistic when SATOBs are included. Other areas where the SATOBs have a notable effect on the non-divergent flow are over the equator, especially over the West Atlantic, where the observations reduce the analysed wind strength and make the flow slightly smoother; and over South-West Africa, where the flow reported by the SATOBs is evidently more complicated than is suggested by the analysis that omitted them.

4.4 Experiment IA4: SATEMs and SATOBs omitted

This experiment used an observing system which may be regarded either as a complete system with satellite temperatures and cloud winds taken away or else as the land-based system (see IA7) with aircraft

reports added on. The assimilation was run with the data from this amended observing system from Day-2 to Day 0 and a forecast was then run forward for 6 days from the analysis for Day 0.

Difference charts for the Atlantic case showing the departure of the height and wind fields from the control assimilation at Day 0 and from the control forecast at Day 3 are shown in Figure 10. These difference patterns may easily be understood by reference to the corresponding charts for IA2 and IA3 (Figs 5 and 8). The major differences of the individual analyses may still be detected in IA4 but the positive height difference just south of 30 N at 45 W has not appeared before. By Day 3 of the forecast however, the difference fields show a pattern which is very like the one which is generated by the addition of the corresponding fields from IA2 and IA3. All the features of the pattern are reproduced in the combined version, but not with the same intensity. On inspection of the difference pattern over the whole globe, it is apparent that there is widespread agreement between the results of IA4 and the combined fields of IA2 and IA3, although there are some areas, mostly over the Pacific, where there is no agreement, even at Day 3. It may be concluded that a linear combination of the results of IA2 and IA3 is a good approximation to those of IA4 although some non-linearities are also present. The success of the combination of the difference fields is probably assisted by the distribution, not just of the two types of observations, but more especially of their impacts, which have their maximum values over different regions of the globe.

4.5 Experiment IA5: AIREPs omitted

In this experiment all types of aircraft reports (AIREPs, ASDAR, AIDS) and reports from Constant Level Balloons were omitted from the observing system. Although the experiment was run just as the others, with an assimilation from Day-2 to Day 0, followed by a 6-day forecast, all the notable results occurred in the first 24 hours after Day 0.

4.5.1 Australian case

At Day 0 a weak surface trough (Fig 4b) over the Great Australian Bight was supported by a closed vortex at 250 mb. A few aircraft reports were made from the vicinity of this vortex, the two most important being just off the coast near 120°E and 130°E. The perturbation that results from the omission of these observations from the assimilation is shown in Figure 11a. The wind difference field is in balance with the height difference field even at analysis time. The whole pattern shows the familiar high-low dipole in the height structure, possibly with some interference on its northern side due to observations over the Australian mainland. The main flow of the wind difference is in opposition to the actual (westerly) wind at 250 mb, showing that the omitted observations helped to enhance the strength of the jet in the analysis. However, the difference field loses its strength quite rapidly; the height difference is halved after 12 hours (Fig 11b) and thereafter is not significant; and although the wind difference declines more slowly, by 24 hours this too is negligible.

4.5.2 North Atlantic Case

Over the North Atlantic the density of AIREPs, including the automatic reporting devices, is the greatest to be found over the whole globe. The effect of the observations at analysis time is clearly to be

seen along the flight paths used on this day: the difference fields are balanced and confirm that the reports have enhanced the strength of the upper flow (Figure 12a). Nevertheless, after 12 hours of the forecast, this impact has already been greatly reduced (Figure 12b), and by 24 hours it has dissipated almost completely, leaving only weak corrections over the circulation of the depression already discussed in IA2 and IA3.

4.6 Experiment IA6: Drifting buoys omitted

In this experiment the reports of surface pressure from drifting buoys were omitted. Analyses were obtained for this depleted observing system from Day-2 to Day 0 and a forecast was then run to Day 6. Inspection of the zonal rms height difference field confirms that all the impact occurs in the Southern Hemisphere (Figs 13a, b).

At Day 0 there are differences of up to 10 mb in individual features of the pmsl field. They are correlated with the control analysis in a manner characteristic of a lack of deepening of lows, or of timing errors in their movement, when the buoy observations are omitted. The difference pattern thus indicates a beneficial impact from these observations. The zonal cross-section (Fig 13a) shows that this impact was communicated to other levels: this is the result of the use of hydrostatic increments over each observation of surface pressure. By Day 3 of the forecast, the impact was carried northwards (Fig 13b) to the equatorial side of the main jet. Meanwhile another part of the impact spread southwards over Antartica, but this area is complicated by the underlying topography and will not be discussed further.

The effect of the buoys is illustrated by the case shown in Figure 14a, which gives the difference field at 250 mb over the Southern Indian Ocean at Day 0. The ill-defined feature in the pmsl field at

50S,20E has already been noted (Section 4.1) and the difference field at 250 mb is just as slack over the same area. However although the forecast traces this feature quite accurately over the subsequent three days, the difference pattern (Figure 14b) shows that in the absence of buoys the forecast was too slow, placing the centre at 80 E, rather than 90 E, on Day 3. Even though the buoy observations are strictly single-level data it is evident that they can be used in a way that has a much longer-lasting impact than other single-level data.

4.7 Experiment IA7: Surface-based Systems only

Most of the satellite-dependent systems (ie SATEMs, SATOBs, AIREPs and COLBAs) were omitted in this experiment, leaving only surface observations of all types - including drifting buoys - and radiosonde reports. The experiment was carried out as before, with assimilations from Day-2 to Day 0 followed by a forecast to Day 6.

As shown in Table 1, the difference in the total observing system between IA7 and IA4 is the same as between IA5 and IA0 (and IA1): the aircraft reports have been withdrawn. However, the IA7/IA4 pair differs from IA0/IA5 by the further absence of SATEMs and SATOBs. Because the impact of AIREPs dies away rather quickly, these differences are more significant in the analysis than in the forecast. (The difference fields at Day 3 in IA7, Figure 15b are similar to the corresponding fields from IA4, Figure 10b).

At analysis time there are features in the difference fields (Fig 15a) which recall previous experiments and which may therefore be ascribed to the omission of one system, independent of the others. The deep height difference near (30 N, 30 W) may be ascribed to the removal of satellite observations (compare Figure 10a from IA4) and the strong

wind difference near (45 N, 30 W) may be ascribed to the removal of AIREPs (compare Figure 12a from IA5). But the peak in the height difference field near (30 N, 40 W) has not been seen before in either IA4 or IA5. It is evident that despite the removal of observations to set up these earlier experiments, there were still enough observations left to affect this area; and that IA7 is the first experiment in which all the observations have been removed from the area. The large impact demonstrates that AIREPs can be very effective in the absence of other data. In this context such a result illustrates the advantages of redundancy in the observing system.

But the difference between IA7 and IA0 at analysis time should also be considered from the original point of view, namely the omission of all three space-based observing systems. The difference field as a whole (Fig 15a) obviously shows a high-low pattern due to a phase error, the result of the main upper low being too far advanced in IA7. There is a notable difference between this phase error and the one found in IA6: here the removal of all upper-air data has produced the error at upper levels at analysis time, but it disappears in the subsequent forecst (Fig 15b). In IA6 however, the removal of surface observations from buoys had less effect on the analysis but it produced a phase error at all levels in the forecast. It seems likely that the retention of surface data in the current experiment, IA7, has had a beneficial effect on the forecast at upper levels as well as at the surface.

4.8 Experiment IA8, Space-Based Systems Only

All surface-based reports were omitted from the observing system for this experiment. All radiosonde reports, surface wind observations and drifting buoy reports were omitted. The observing system that was left

was entirely made up of devices that are satellite-dependent. The established procedure of two days of assimilation and six of prediction was carried out for this system.

In this experiment the only information that is available for the individual observing systems omitted comes from IA6, the run without drifting buoy observations. On inspection it can be seen that the difference patterns over the Southern Hemisphere (not shown) do indeed show a similarity between IA6 and IA8, except where sonde reports from South America and Australasia have had a significant effect.

But the most obvious feature of the difference fields is found over the North Atlantic. In the control assimilation (IAO) the surface depression initially over the east coast of the USA, and its subsequent movement North and East, have been noted (Fig. 4). The difference fields at 250 mb for the current experiment show that the associated upper circulation is in error at Day 0 (Fig. 16a), and that as the forecast proceeds this error develops further (Fig. 16b) so that by Day 3 the British Isles are engulfed by a major error, corresponding to a considerable over-deepening of the upper vortex. It is perhaps surprising that there is no similar erroneous development over the Pacific. However, although there is a low off Japan at Day 0, the whole system is over the sea and not over land. This area would have been covered by SATEMs (which are used over sea but not over land) whereas the Atlantic system started off over the land-mass of North America and would have had no supporting observations during the assimilation period. The results of this experiment thus illustrate the important role of sonde and surface reports and also the dependence of impact studies on the synoptic situation.

5. ROOT MEAN SQUARE DIFFERENCES

The experiments described in Section 4 have revealed a number of interesting features as they developed out of a single global synoptic situation. The cases that have been described were selected for their relevance to a particular phenomenon or simply for the size of the observational impact, large or small. While the various cases show qualitative results of some significance, no quantitative results have been obtained.

A conventional measure of model accuracy is the root mean square (rms) difference between a forecast field and its verifying analysis. By computing such rms differences, with the mean taken over all model points, we may generate a set of numbers which measure at least one aspect of the performance of the various observing systems over the globe as a whole. However, although the presentation of results in this form enables comparisons to be made between the various experiments, the effect of taking a global average is to spread out the impact of an individual sub-system. In fact the global rms differences use the same differences for each model row that went into the zonal cross-sections given in the previous section. The global values are thus a broad summary of each experiment and they should include the synoptic-scale effects already discussed.

In the course of this Section, rms differences will be presented for most of the experiments reported in Section 4. In general, it is expected that rms departures from the control analysis will increase when observation systems are removed: thus, during the forecast period the

value of |IAn - IAO| (n = 2 to 8) is expected to be greater than |IA1 -IAO|. Such a result implies that the system withdrawn in experiment IAn had a beneficial impact when included in the control runs.

Some rms differences from IA2 at Day 3 are given in Table 2a and b. The triangles in Figures 17a and b have been drawn with the vertices to represent one of the three model states, IAO (the control analysis), IA1 (the control forecast) and IA2 (the forecast from a depleted set of observations), and sides of the triangles proportional to the rms differences between the states at each end, as given in the Tables. The triangles for four different levels, Figure 17a, are seen to have very similar shapes: although the magnitude of the forecast-analysis difference increases up to 250 mb, the angles of the triangles do not show much change. The angle at the vertex F_2, corresponding to the forecast from IA2, is such that its cosine is the correlation coefficient between the forecast difference, F_1F_2, and the forecast-analysis difference when the observations (SATEMs) are omitted, F_2A_o. This correlation is a measure of the usefulness of the observations. If the angle at F_2 is small, F_1F_2 is well-correlated with F_2A_o, implying that the full forecast, F_1, has reduced the errors in F_2. On the three tropospheric levels the magnitude of the correlation is nearly constant (Table 2a), at a value of about 0.33, but it drops to 0.23 at 100 mb. This pattern is repeated in all the experiments, except one, IA6 (DRIBUs omitted), where the increase of correlation with height is much stronger than in IA2. These results confirm that the impact at the 250 mb level may be regarded as typical of the whole troposphere in these studies.

The triangles in Figure 17b show three sets of rms differences for different regions of the globe, as given in Table 2b. They indicate that although the magnitude of the differences may be ranked in the familiar order Southern Hemisphere > Northern Hemisphere > Tropics, the angles at F_2 in the triangles for each region are about the same, as shown by the correlation coefficients in Table 2b. If there is any significance in the differences between these correlations, they suggest that, in this instance, the SATEMs are most useful in the Southern Hemisphere and that their relative benefit in the Tropics is virtually the same as in the Northern Hemisphere. Comparison between the regions in this manner is only possible where there is a uniform cover of data over the whole globe. However the figures in both Tables 2a and b do clearly show that some important results may be obtained by considering not just the magnitudes of the differences but also their correlations.

In view of the similarity of the triangles from one level to another over the globe, and from one region to another on one level, it is reasonable to summarize the results of the experiments as a set of rms differences for one level, 250 mb, over the whole globe. These are presented in Table 3a for heights and Table 3b for winds, at Day 0 and for three days during the forecast. The correlations of the forecast difference with the forecast-analysis difference are given in Table 3c for Days 1 and 3 only: beyond Day 3 the correlations are too small to suggest any degree of usefulness.

6. DISCUSSION

Some broad conclusions may be drawn from the results of the previous Sections.

The rms differences in Tables 3a, b indicate that the impact of SATEMs shown by experiment IA2 has been beneficial when taken overall. This is consistent with the results of the much more extensive studies of Halem et al (1982) on the impact of satellite data during SOP-1, and it suggests that the detrimental effects observed in parts of the Southern Hemisphere are compensated by beneficial effects elsewhere in the same hemisphere and in the Northern Hemisphere. This sub-system is the dominating contribution to IA4 and IA7, and in all three experiments the Tables show the benefit of the SATEMs continuing right through the forecast to Day 6. The rms differences due to the buoys in IA6 are diluted by the global averaging, and in addition, they are initiated as perturbations at the surface: consequently, the differences at analysis time are small, but the impact at 250 mb is to be seen well into the forecast period. Of all the experiments, IA8, where radiosondes are the principal sub-system removed, and which showed the most dramatic differences in the cases studied in Section 4, has the largest rms differences by Day 3 of the forecast, confirming the beneficial impact of the surface-based data.

The global rms differences from IA3 suggest that satellite wind observations have only a small impact which is not always beneficial. On investigation this appears to be the result of a part of the analysis program where a choice is exercised in the selection of data. When SATOBs are excluded, other data may be taken into consideration. This effect is worst in the areas with a high density of data, most obviously the middle latitudes of the Northern Hemisphere. Fortunately the cases studied in 4.3 are from areas with a relatively low density of data and

are unlikely to be affected by this fault, but rms differences taken over the globe are obviously affected and so they have been omitted from the tables.

The data-selection routine also seems to have had an adverse effect on the impact of aircraft reports in IA5, although not so severely as in IA3. The effect is confirmed when the comparison of the pair (IA7, IA4) with (IA5, IA1(0)) is extended to quantitative results. Of the cases studied in 4.5, only the North Atlantic is likely to be much affected, but the general behaviour is not misleading since the rapid decay of data impact is a feature of both qualitative comparisons. However the discussion of the results from the later stages of IA5 require a more detailed treatment than can be accommodated here and so these results have also been omitted.

The generally low values of the correlation coefficients in Table 3c should be noted. Although the SATEMs have produced high values in IA2, 4 and 7 on Day 1, only IA8 remains above 0.5 on Day 3. It is believed that the low values are symptomatic of a fundamental difficulty in obtaining useful meteorological data. It is apparent that analysis errors occur in certain areas and subsequently propagate into the forecast. In considering a single synoptic situation, as has been done here, the most effective use of the observing systems would be to direct them to the areas where they may prevent the major analysis errors from occurring. But most of the systems are automatic and we have little control, if any, over the location of the data. The low correlations may be a reflection of this randomness in the FGGE data distribution.

7. ACKNOWLEDGEMENTS

I am grateful to Brian Barwell and Angela Smith for their assistance and industry at various stages of this work.

REFERENCES

Barwell, B.R. and A. Lorenc, 1985: A study of the impact of aircraft wind observations on a large-scale analysis and numerical weather prediction system. To be published in Quart. J. R. Met. Soc.

Bell, R.S., 1983: The Meteorological Office operational global data assimilation and forecast system. Am. Met. Soc., 6th Conference on Numerical Wether Prediction, Omaha, USA.

Bjorheim, K., P. Julian, M. Kanamitsu, P. Kallberg, P. Price, S. Tracton, and S. Uppala, 1981: The Global Weather Experiment, daily global analysis. Published by ECMWF.

Foreman, S.J., 1983: The Numerical Weather Prediction Model of the Meteorological Office. Am. Met. Soc., 6th Conference on Numerical Weather Prediction, Omaha, USA.

Halem, M., E. Kalnay, W. E. Baker and R. Atlas, 1982: An assessment of the FGGE satellite observing system during SOP-1. Bull. Am. Met. Soc., 63, 407-426.

Hollingsworth, A., A. C. Lorenc, M.S. Tracton, K. Arpe, G. Cats, S. Uppala and P. Kallberg, 1982: The response of Numerical Weather Prediction systems to FGGE II-B data. ECMWF Workshop on Current Problems in Data Assimilation, November 1982, pp 19-125. (Also submitted to Quart J. R. Met. Soc.).

Kashiwagi, K., 1984: On the impact of space-based observing systems in the JMA global forecast/analysis system. This volume.

Tibaldi, S., 1984: Results from the second observing system experiment at ECMWF. This volume.

	SATEMS	SATOBS	AIREPS	DRIFTING BUOYS	SONDES SURFACE SHIPS
IA0, IA1	I	I	I	I	I
IA2	O	I	I	I	I
IA3	I	O	I	I	I
IA4	O	O	I	I	I
IA5	I	I	O	I	I
IA6	I	I	I	O	I
IA7	O	O	O	I	I
IA8	I	I	I	O	O

TABLE 1 Observation types included (I) or omitted (O) for each impact study

TABLE 2a Global results on four pressure levels

	850 mb	500	250	100
IA1-IAO	4.36	5.70	7.56	6.53
IA2-IAO	4.38	6.01	8.06	6.56
IA2-IA1	2.64	3.06	3.87	2.83
Correlation (IA2-IA1, IA2-IAO)	0.31	0.35	0.37	0.23

TABLE 2b Results at 250 mb for four regions

	N. Hemisphere 90N-20N	Tropics 40N-40S	S Hemisphere 20S-90S	Globe 90N-90S
IA1-IAO	6.52	4.07	11.21	7.56
IA2-IAO	6.88	4.31	11.98	8.06
IA2-IA1	2.23	1.73	6.31	3.87
Correlation (IA2-IA1, IA2-IAO)	0.34	0.34	0.38	0.36

TABLE 2 Root mean square height differences (in geopotential decametres) and correlation of difference between forecasts with difference between forecast and analysis, Experiment IA2.

TABLE 3a Global rms differences, 250 mb height (decametres)

		IAn-IAO				IAn-IA1		
	Day	D0	D1	D3	D6	D1	D3	D6
Control f/c	IA1	-	3.71	7.56	9.47	-	-	-
No SATEMs	IA2	2.77	4.67	8.06	10.54	2.76	3.88	5.60
No SATEMS) or SATOBS)	IA4	3.13	4.74	7.94	10.96	3.13	3.92	5.75
No DRIBUs	IA6	0.84	3.90	7.78	10.10	1.09	1.74	3.17
Land-based	IA7	3.30	4.81	8.02	11.14	3.29	4.08	5.95
Space-based	IA8	2.78	4.56	8.82	10.79	2.78	5.15	7.29

TABLE 3b Global rms differences, 250 mb wind (m/s)

		IAn-IAO				IAn-IA1		
	Day	D0	D1	D3	D6	D1	D3	D6
Control f/c	IA1	-	10.69	14.89	18.97	-	-	-
No SATEMs	IA2	5.33	11.77	16.02	19.18	7.44	8.58	11.31
No SATEMs) or SATOBs)	IA4	7.81	12.26	15.49	20.08	9.28	9.60	11.84
No DRIBUs	IA6	1.58	10.87	15.34	19.17	2.40	3.98	6.35
Land-based	IA7	8.57	12.43	15.74	20.14	9.49	9.84	12.13
Space-based	IA8	6.89	11.56	16.64	19.68	8.72	10.61	14.04

Table 3c Coefficient of correlation of (IAn-IA1) with (IAn-IAO)

IAn	IA2	IA4	IA6	IA7	IA8
Day 1	0.61	0.62	0.31	0.64	0.58
Day 3	0.37	0.34	0.24	0.36	0.52

TABLE 3 Global results for individual experiments.

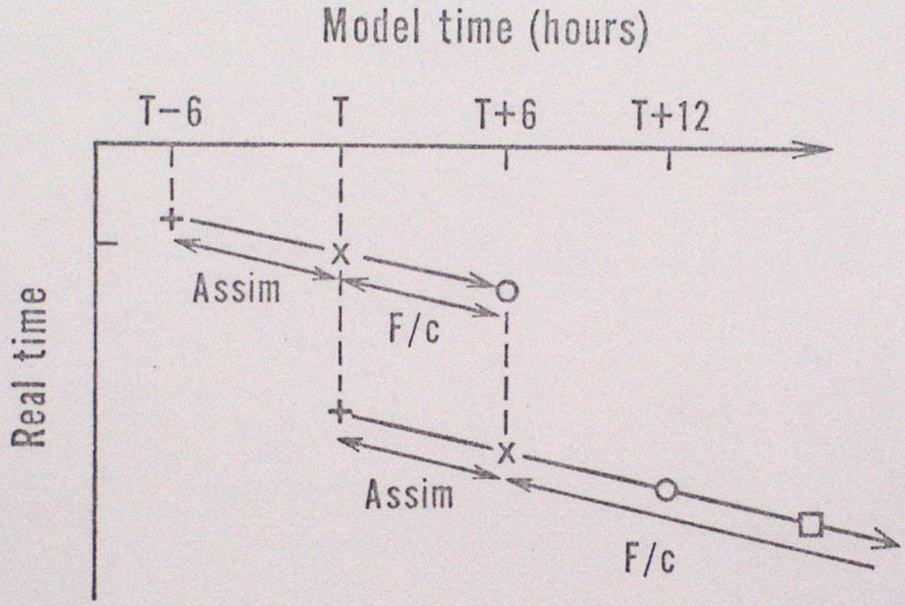

+ = Starting analysis, copy of previous x

x = Analysis after assimilation of data

o = 6-hour forecast, background for next x

□ = Subsequent forecast time

DO 3319

FIGURE 1 A Cycle of the Numerical Model

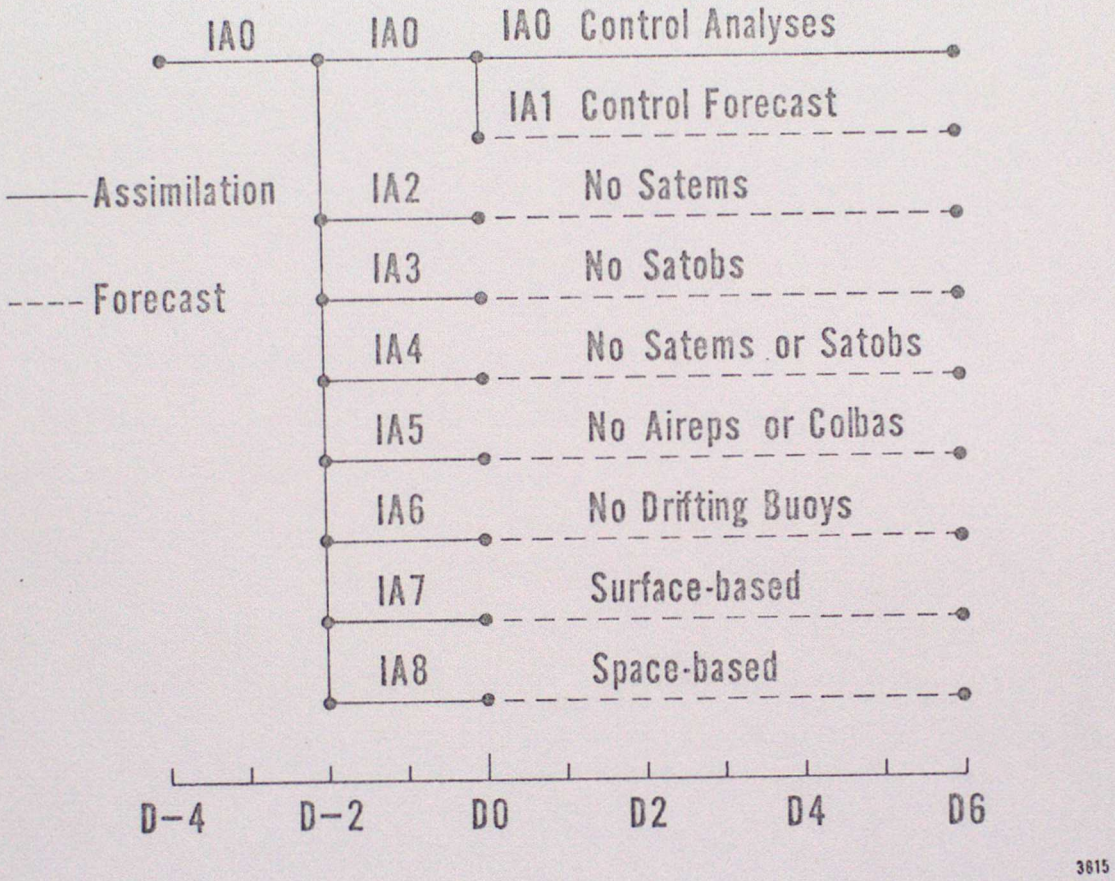

FIGURE 2 The Design of the Impact Studies

a) POSITION OF SATEM OBSERVATIONS
OZ ON 27/2/1979

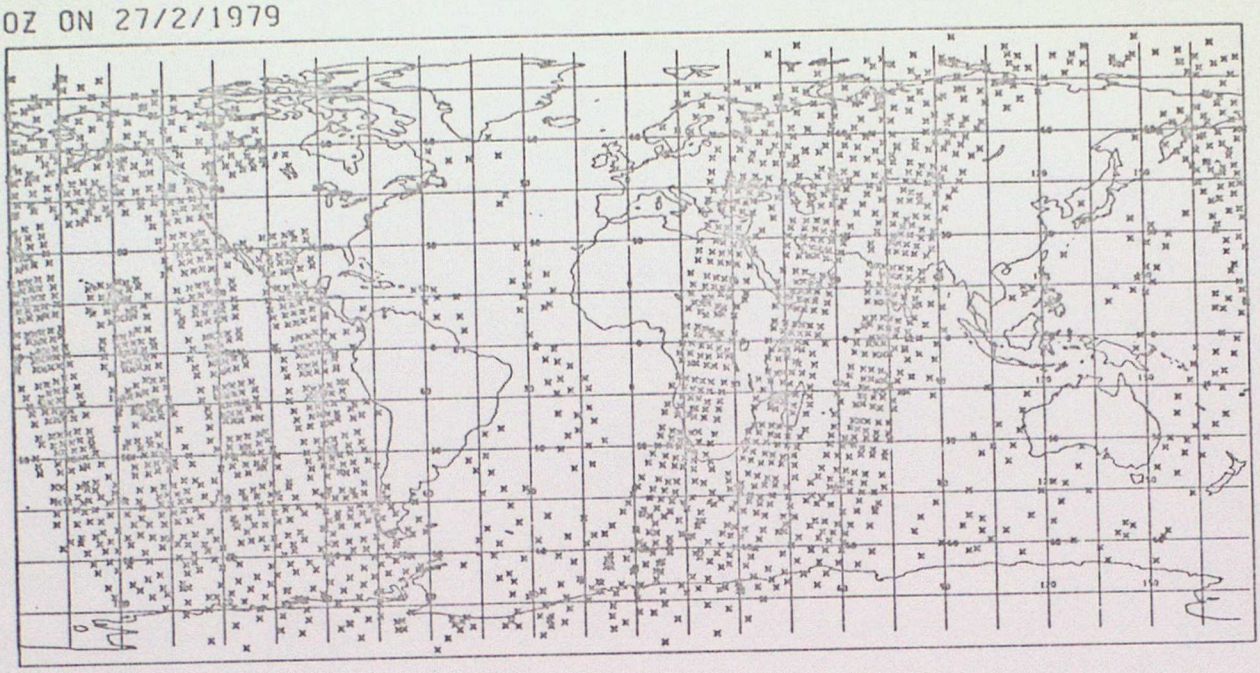

b) POSITION OF SATOB OBSERVATIONS
OZ ON 27/2/1979

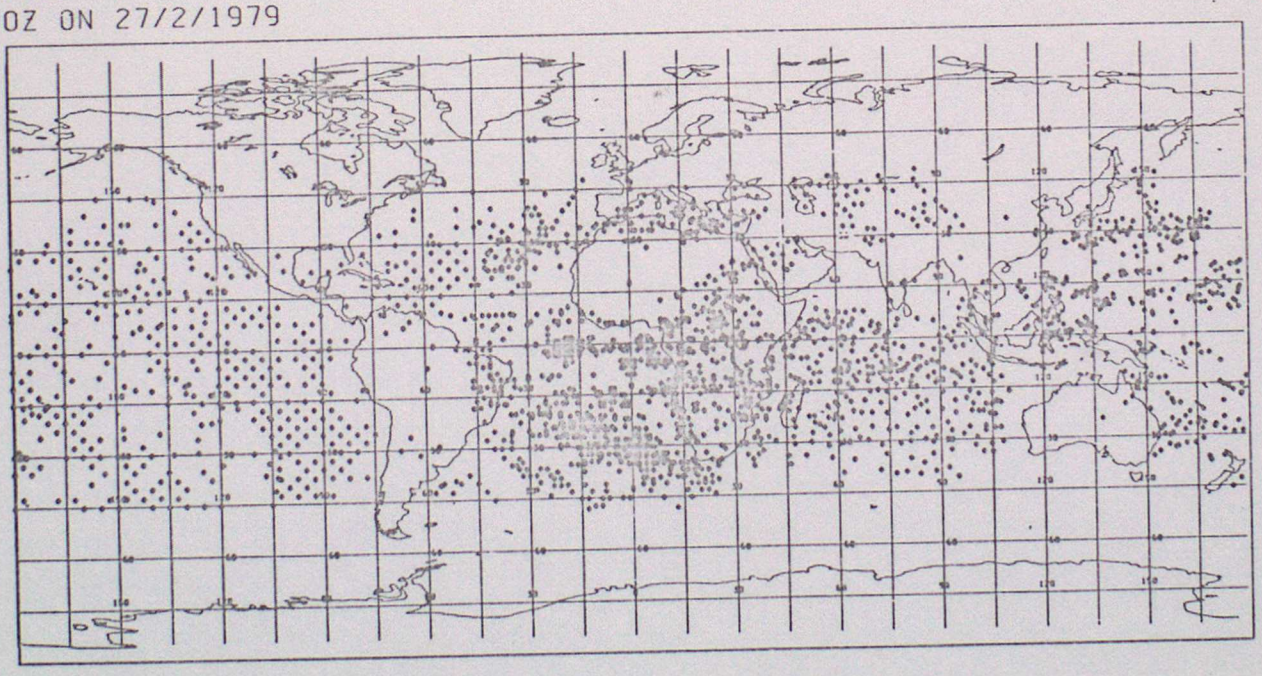

FIGURE 3 The Distribution of Satellite Observations: a) Satems, b) Satobs

EXPERIMENT IAO CONTROL ASSIMILATION
VALID AT OZ ON 27/2/1979 DAY 0
MEAN SEA-LEVEL PRESSURE

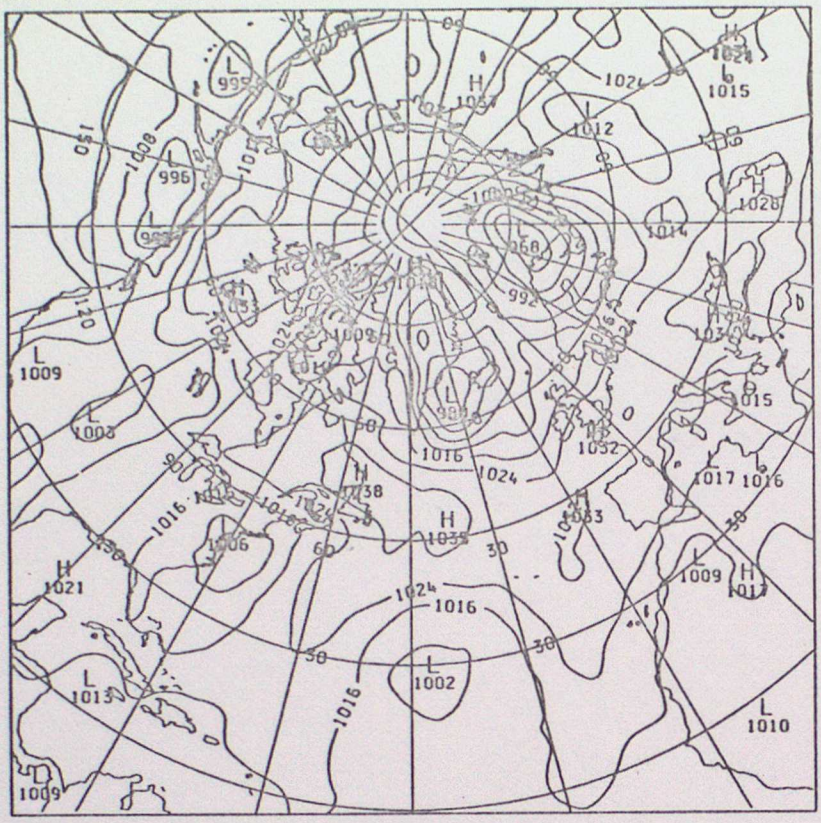

FIGURE 4a

Control Analysis at Day 0, Northern Hemisphere

EXPERIMENT IAO CONTROL ASSIMILATION
VALID AT OZ ON 27/2/1979 DAY 0
MEAN SEA-LEVEL PRESSURE

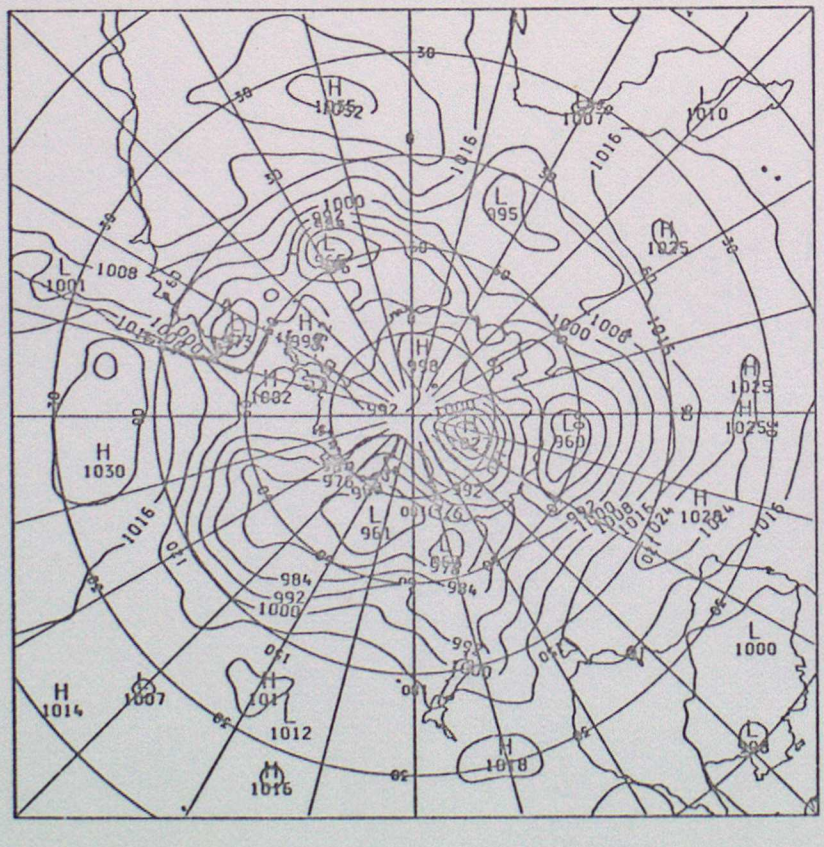

FIGURE 4b

Control Analysis at Day 0, Southern Hemisphere

EXPERIMENT IA0 CONTROL ASSIMILATION
VALID AT 0Z ON 28/2/1979 DAY 1
MEAN SEA-LEVEL PRESSURE

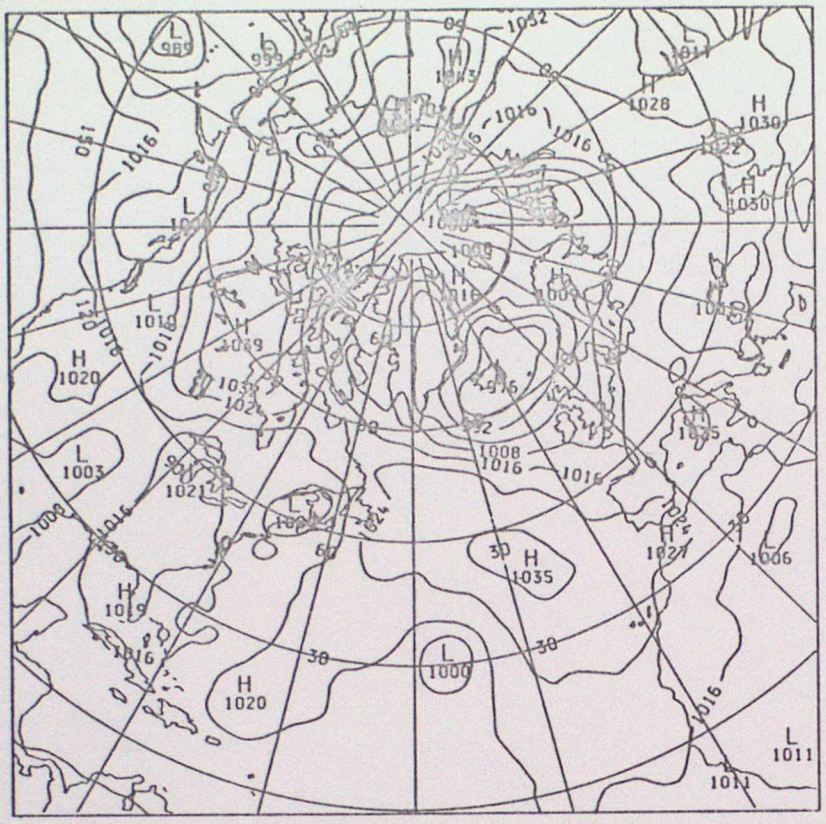

FIGURE 4c
Control Analysis at Day 1, Northern Hemisphere

EXPERIMENT IA1 CONTROL FORECAST
VALID AT 0Z ON 28/2/1979 DAY 1
MEAN SEA-LEVEL PRESSURE

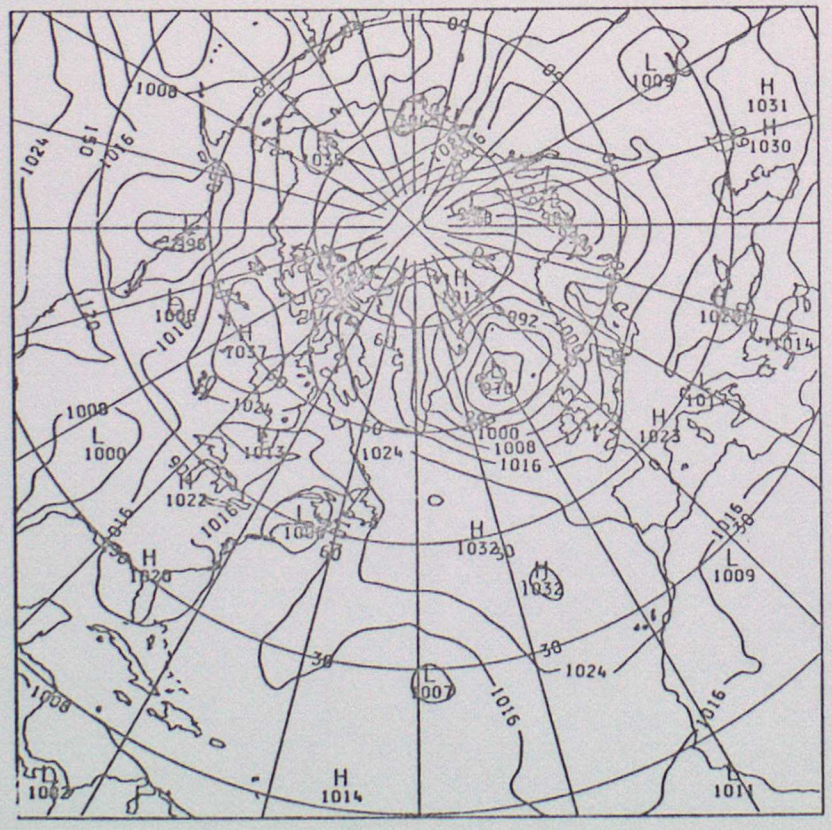

FIGURE 4d
Control Forecast at Day 1, Northern Hemisphere

EXPERIMENT IA0 CONTROL ASSIMILATION
VALID AT 0Z ON 28/2/1979 DAY 1
MEAN SEA-LEVEL PRESSURE

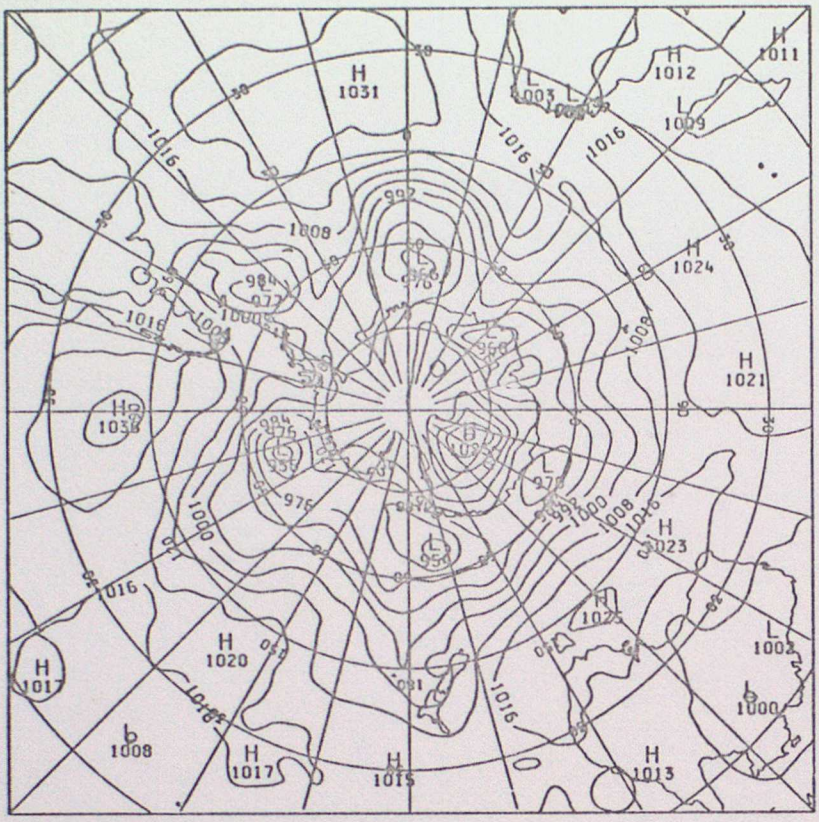

FIGURE 4e

Control Analysis at Day 1, Southern Hemisphere

EXPERIMENT IA1 CONTROL FORECAST
VALID AT 0Z ON 28/2/1979 DAY 1
MEAN SEA-LEVEL PRESSURE

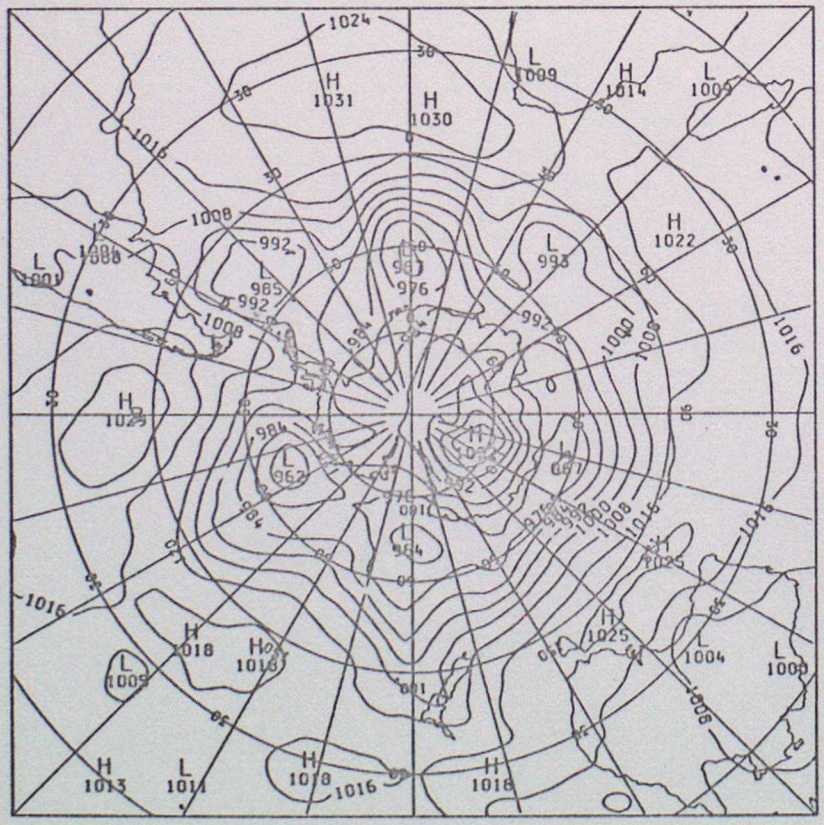

FIGURE 4f

Control Forecast at Day 1, Southern Hemisphere

EXPERIMENT IA0 CONTROL ASSIMILATION
VALID AT 0Z ON 1/3/1979 DAY 2
MEAN SEA-LEVEL PRESSURE

FIGURE 4g
Control Analysis at Day 2, Northern Hemisphere

EXPERIMENT IA1 CONTROL FORECAST
VALID AT 0Z ON 1/3/1979 DAY 2
MEAN SEA-LEVEL PRESSURE

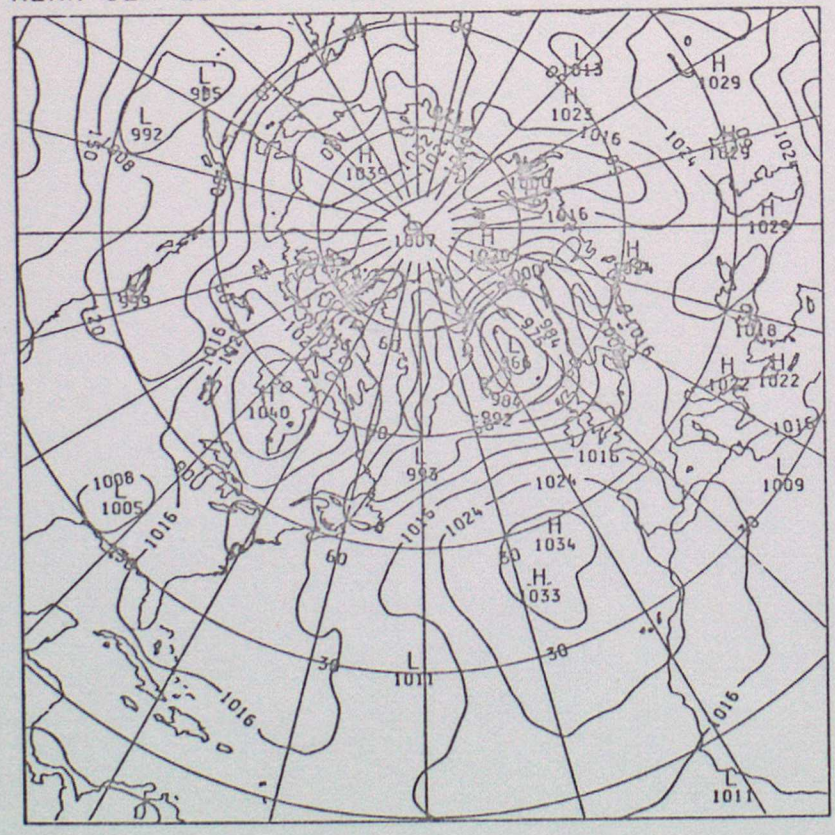

FIGURE 4h
Control Forecast at Day 2, Northern Hemisphere

EXPERIMENT IA0 CONTROL ASSIMILATION
VALID AT 0Z ON 1/3/1979 DAY 2
MEAN SEA-LEVEL PRESSURE

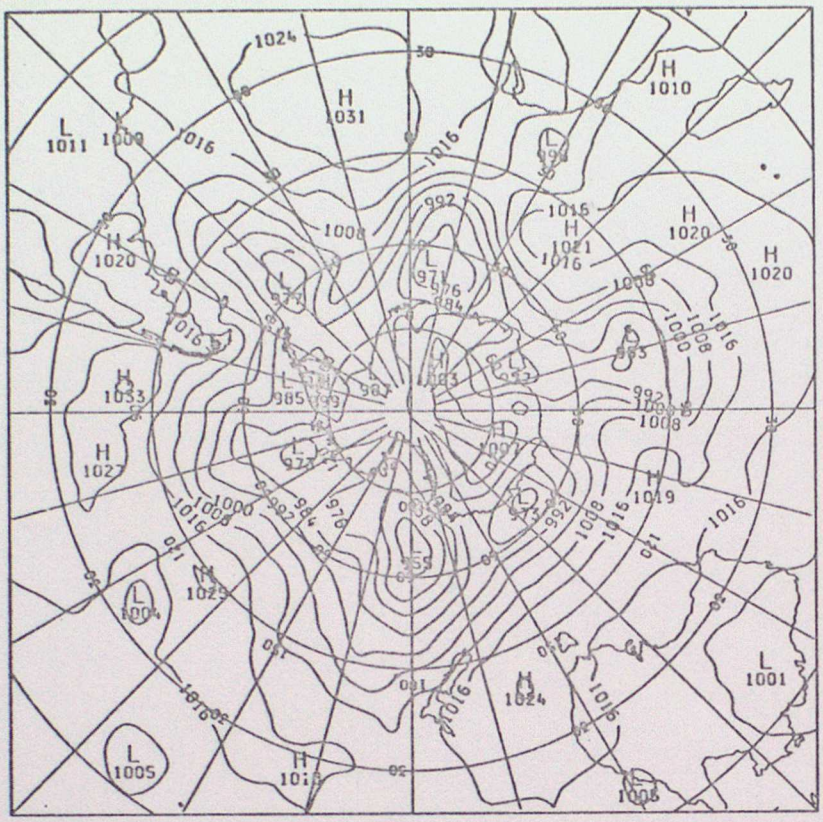

FIGURE 4i

Control Analysis at Day 2, Southern Hemisphere

EXPERIMENT IA1 CONTROL FORECAST
VALID AT 0Z ON 1/3/1979 DAY 2
MEAN SEA-LEVEL PRESSURE

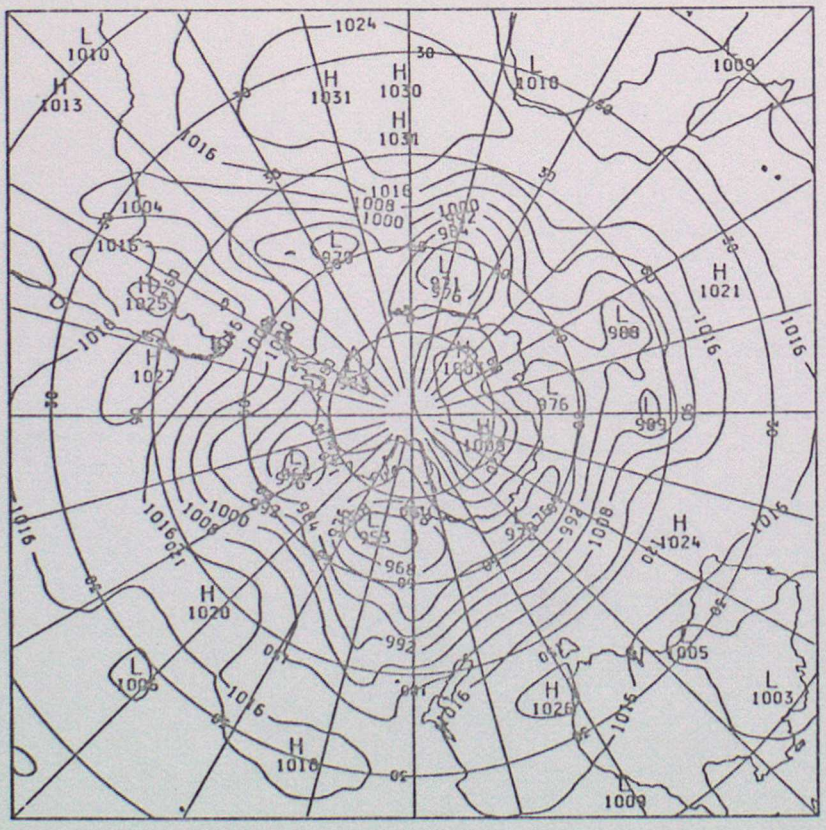

FIGURE 4j

Control Forecast at Day 2, Southern Hemisphere

EXPERIMENT IA0 CONTROL ASSIMILATION
VALID AT 0Z ON 2/3/1979 DAY 3
MEAN SEA-LEVEL PRESSURE

FIGURE 4k

Control Analysis at Day 3, Northern Hemisphere

EXPERIMENT IA1 CONTROL FORECAST
VALID AT 0Z ON 2/3/1979 DAY 3
MEAN SEA-LEVEL PRESSURE

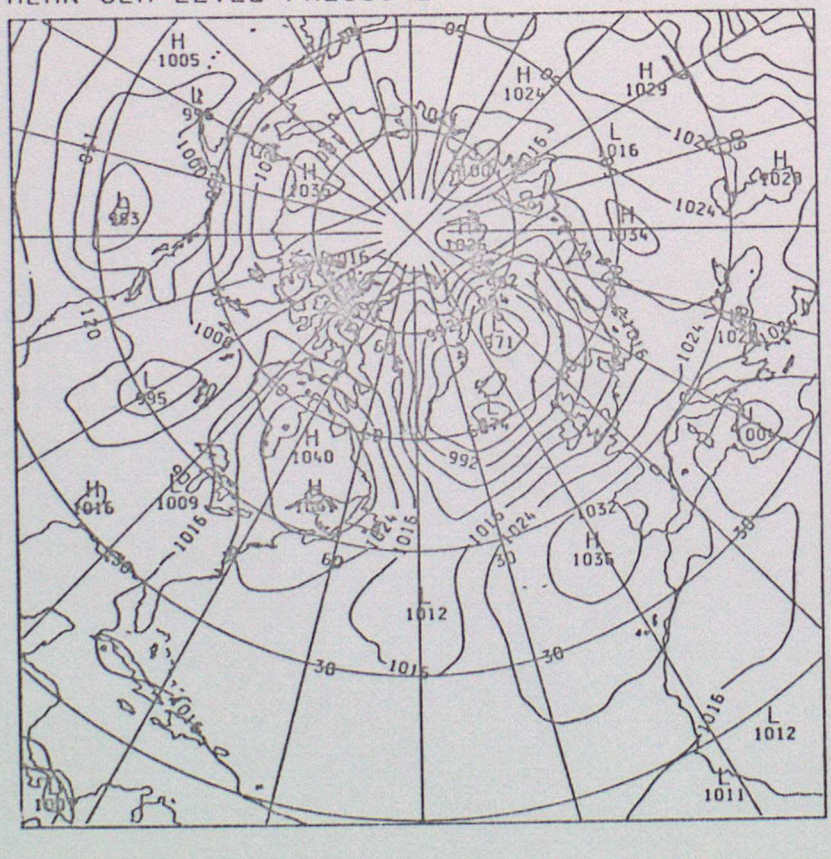

FIGURE 41

Control Forecast at Day 3, Northern Hemisphere

EXPERIMENT IA0 CONTROL ASSIMILATION
VALID AT 0Z ON 2/3/1979 DAY 3
MEAN SEA-LEVEL PRESSURE

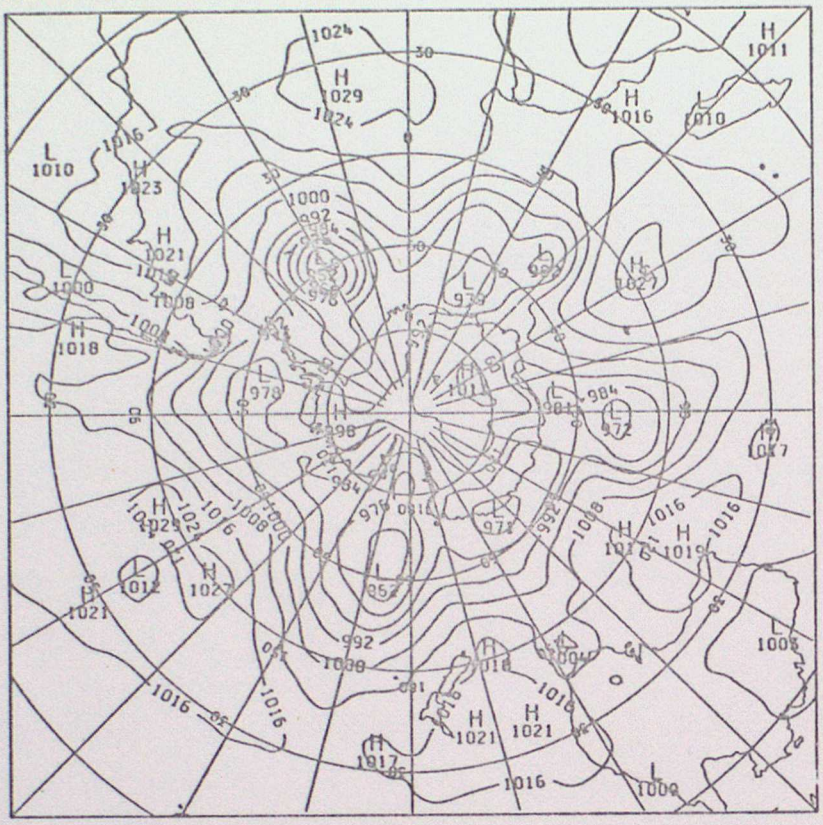

FIGURE 4m

Control Analysis at Day 3, Southern Hemisphere

EXPERIMENT IA1 CONTROL FORECAST
VALID AT 0Z ON 2/3/1979 DAY 3
MEAN SEA-LEVEL PRESSURE

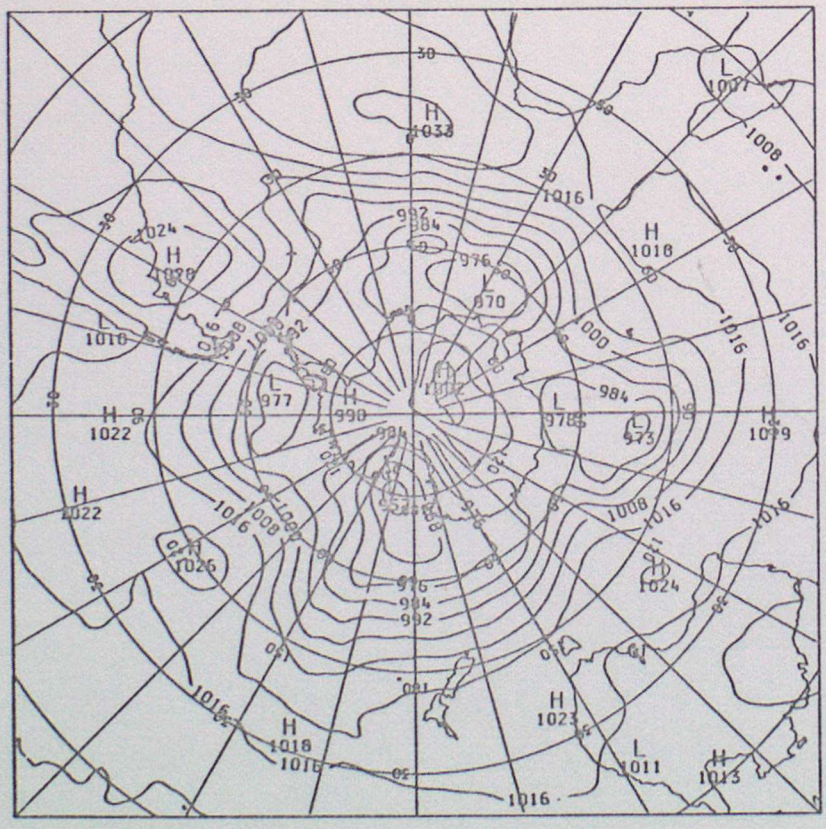

FIGURE 4n

Control Forecast at Day 3, Southern Hemisphere

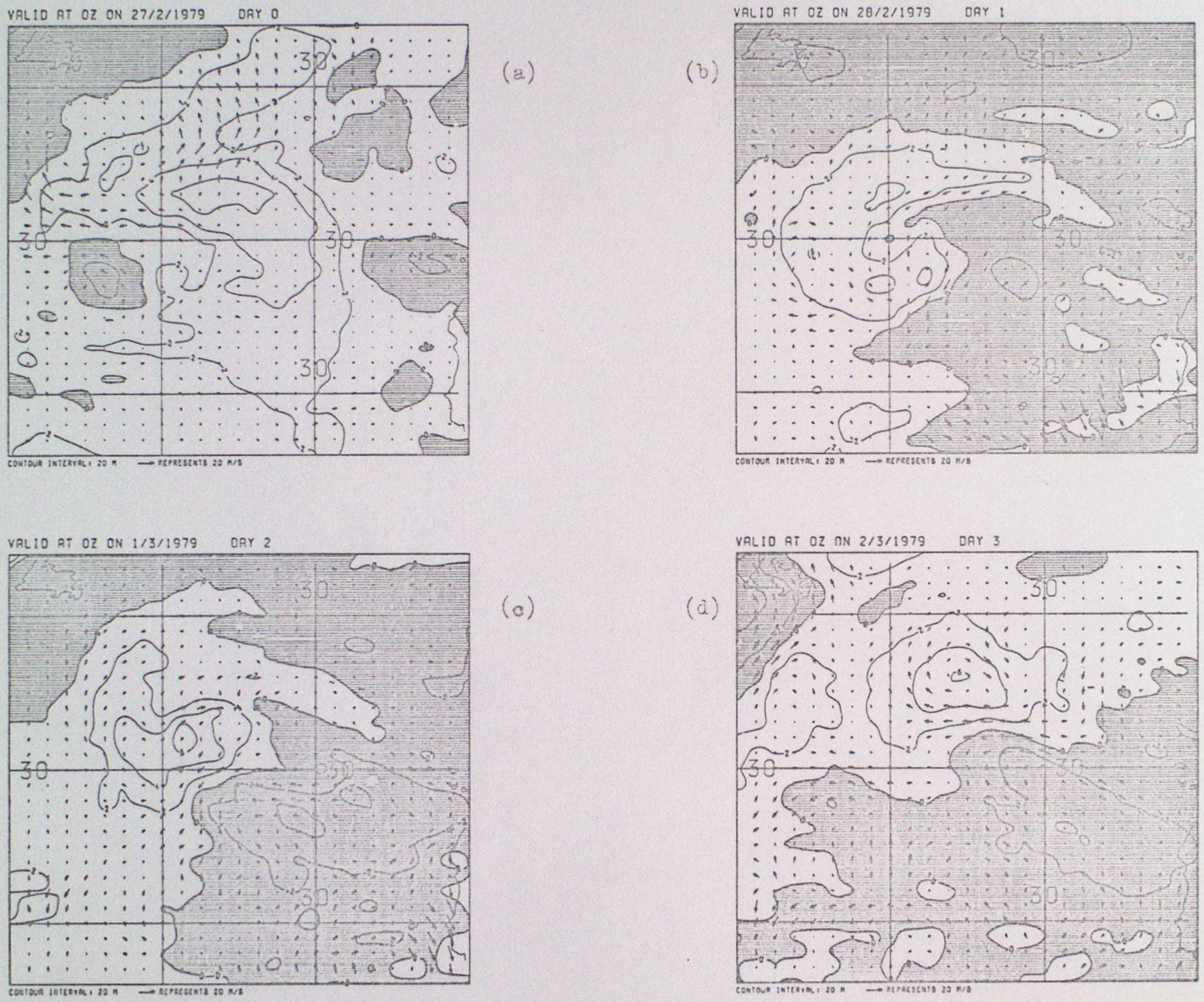

FIGURE 5

Height and Wind Differences at 250mb, N.Atlantic

a) IA2 - IA0, Day 0

b) IA2 - IA1, Day 1

c) IA2 - IA1, Day 2

d) IA2 - IA1, Day 3

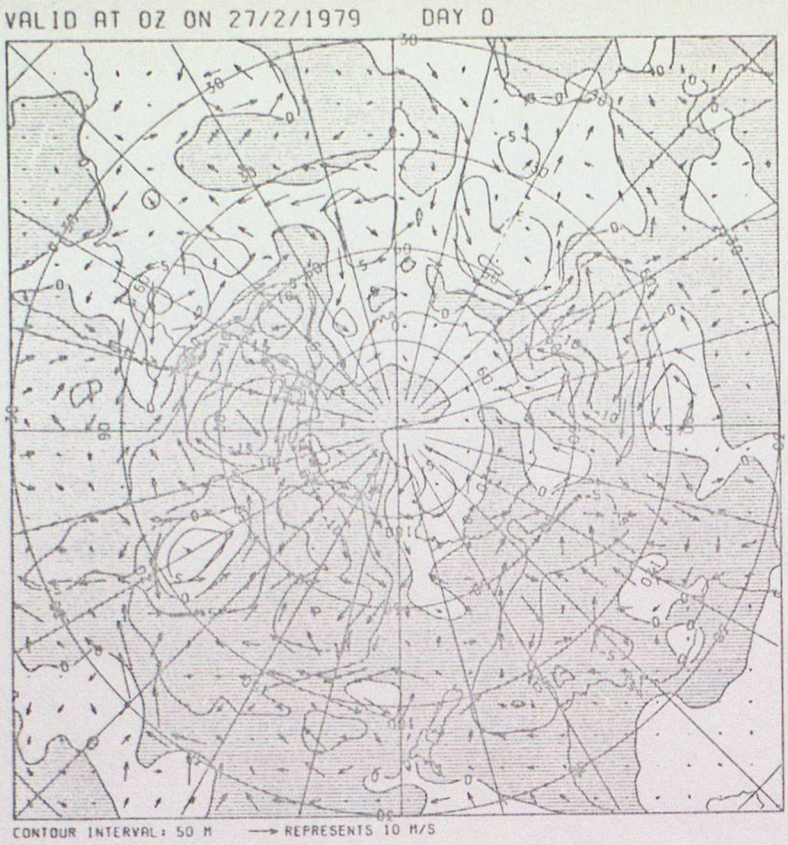

FIGURE 6a

Height and Wind Differences at 250mb, IA2 - IA0, Day 0, Southern Hemisphere

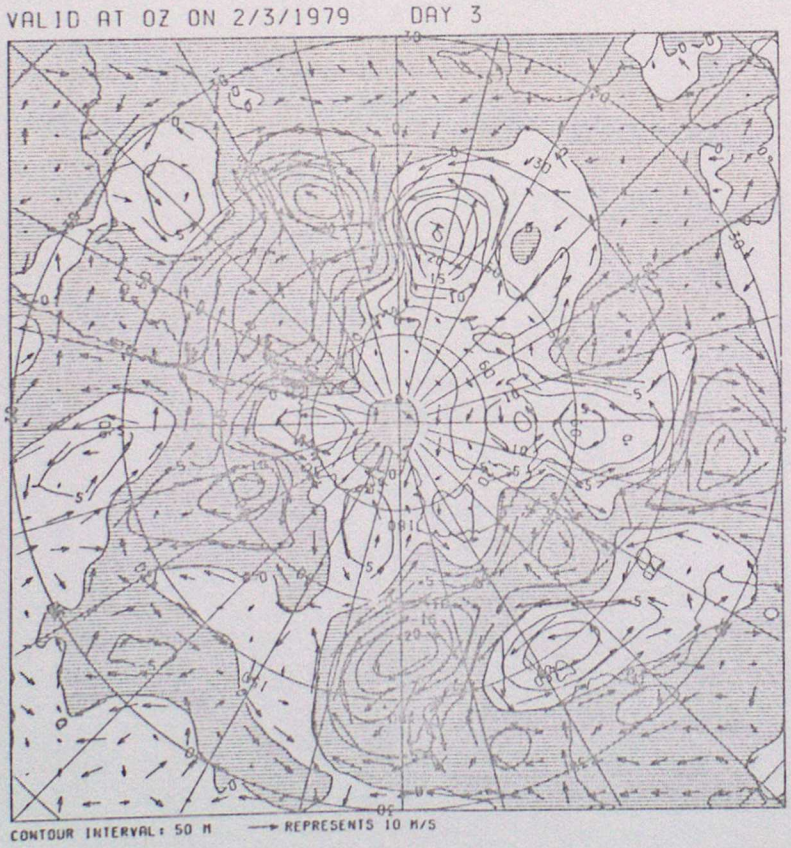

FIGURE 6b

Height and Wind Differences at 250mb, IA2 - IA1, Day 3, Southern Hemisphere

EXPERIMENT IA0 (CONTROL ASSIMILATION)
GEOPOTENTIAL HEIGHT AT 500 MB + 1000-500 THICKNESS
VALID AT 0Z ON 27/2/1979

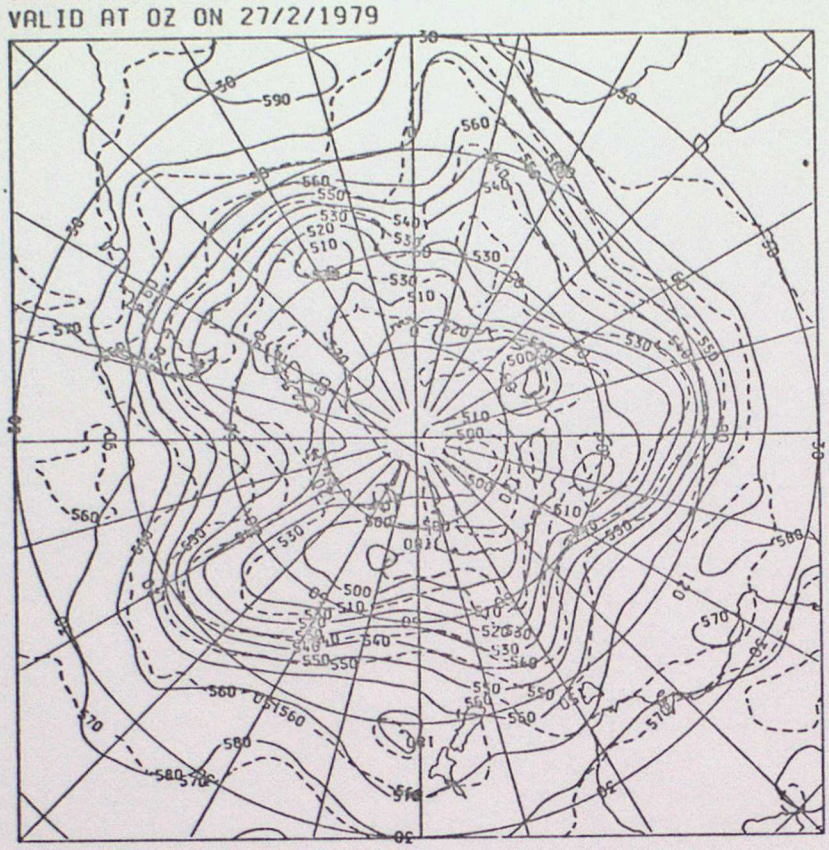

FIGURE 6c

Analysed 500mb Height and 1000 - 500mb Thickness, Control Analysis, Day 0, Southern Hemisphere

EXPERIMENT IA2 (NO SATEMS)
GEOPOTENTIAL HEIGHT AT 500 MB + 1000-500 THICKNESS
VALID AT 0Z ON 27/2/1979

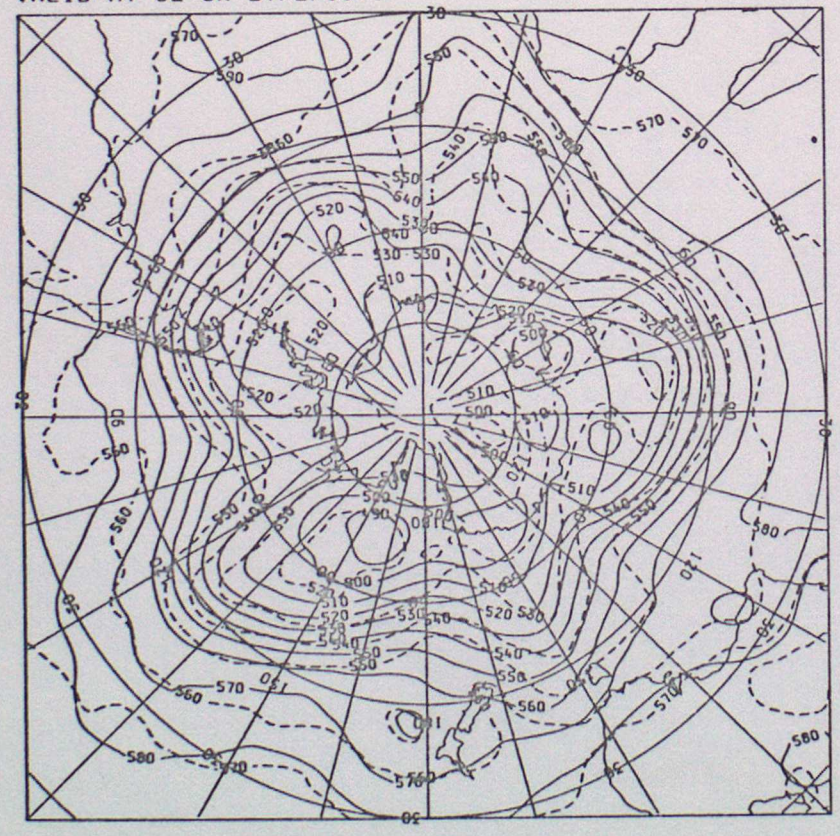

FIGURE 6d

Analysed 500mb Height and 1000 - 500mb Thickness, Impact Study IA2 (No Satems), Day 0, Southern Hemisphere

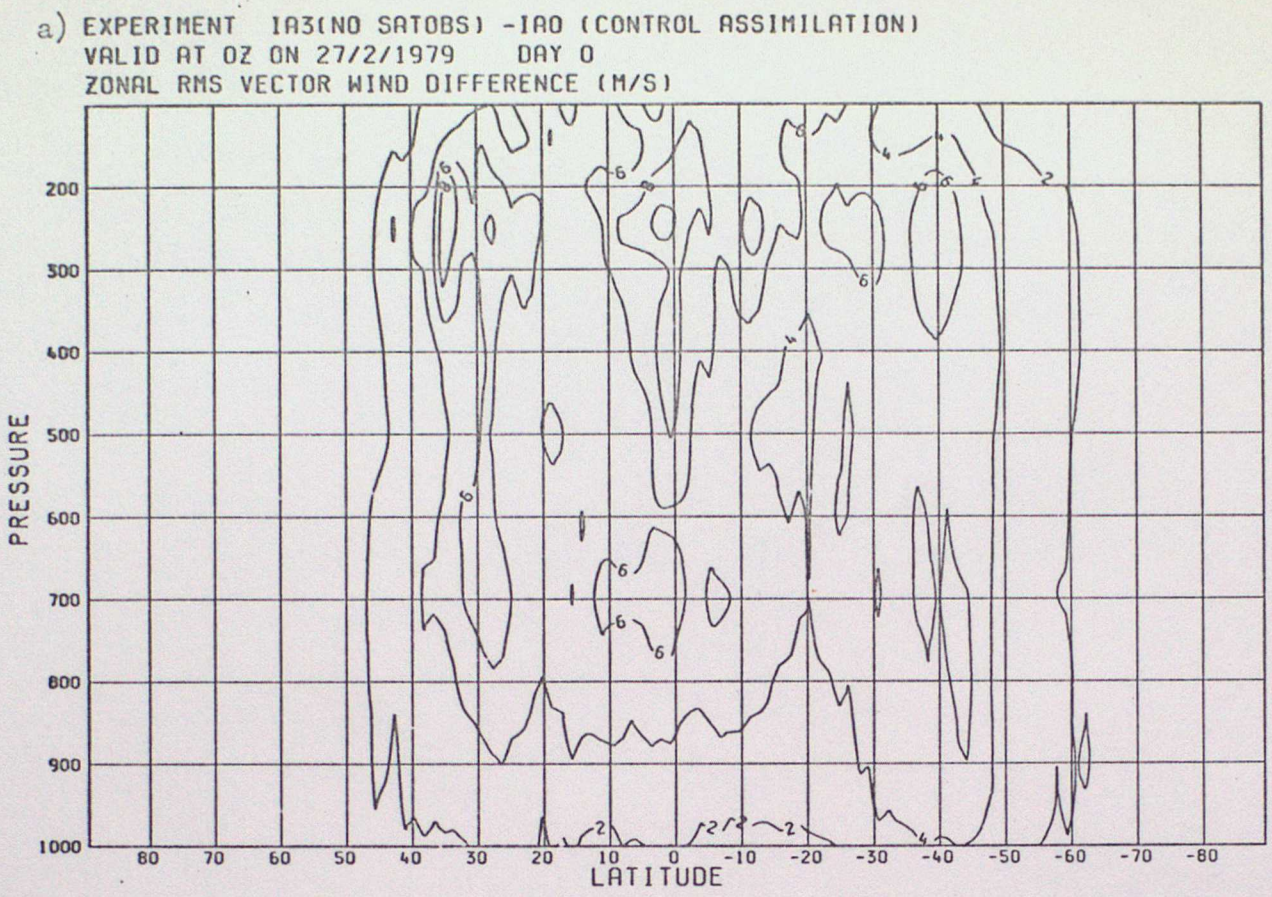

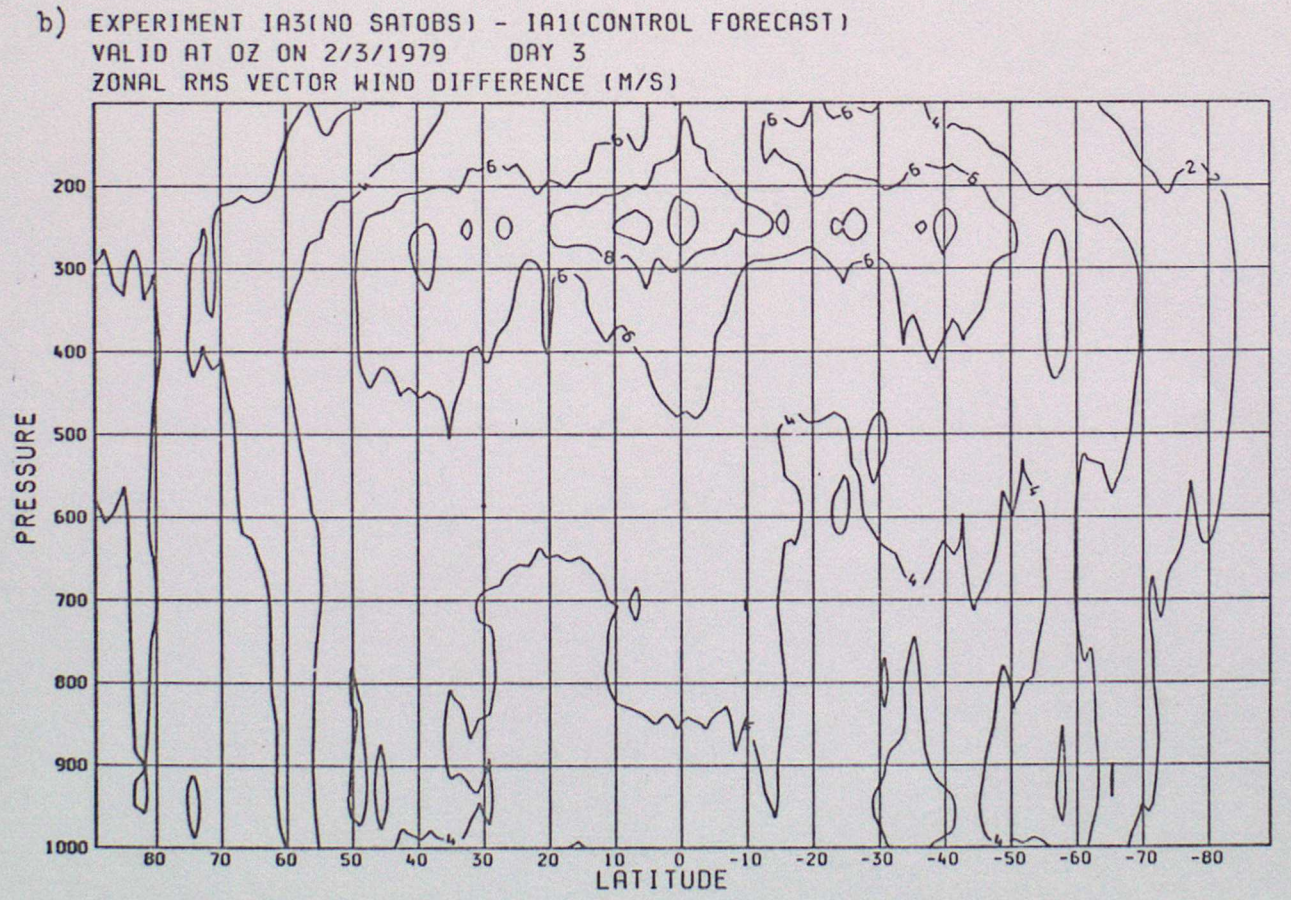

FIGURE 7 Zonal Cross-Sections of rms Vector Wind Differences, Impact Study IA3(No Satobs): a) Day 0, b) Day 3

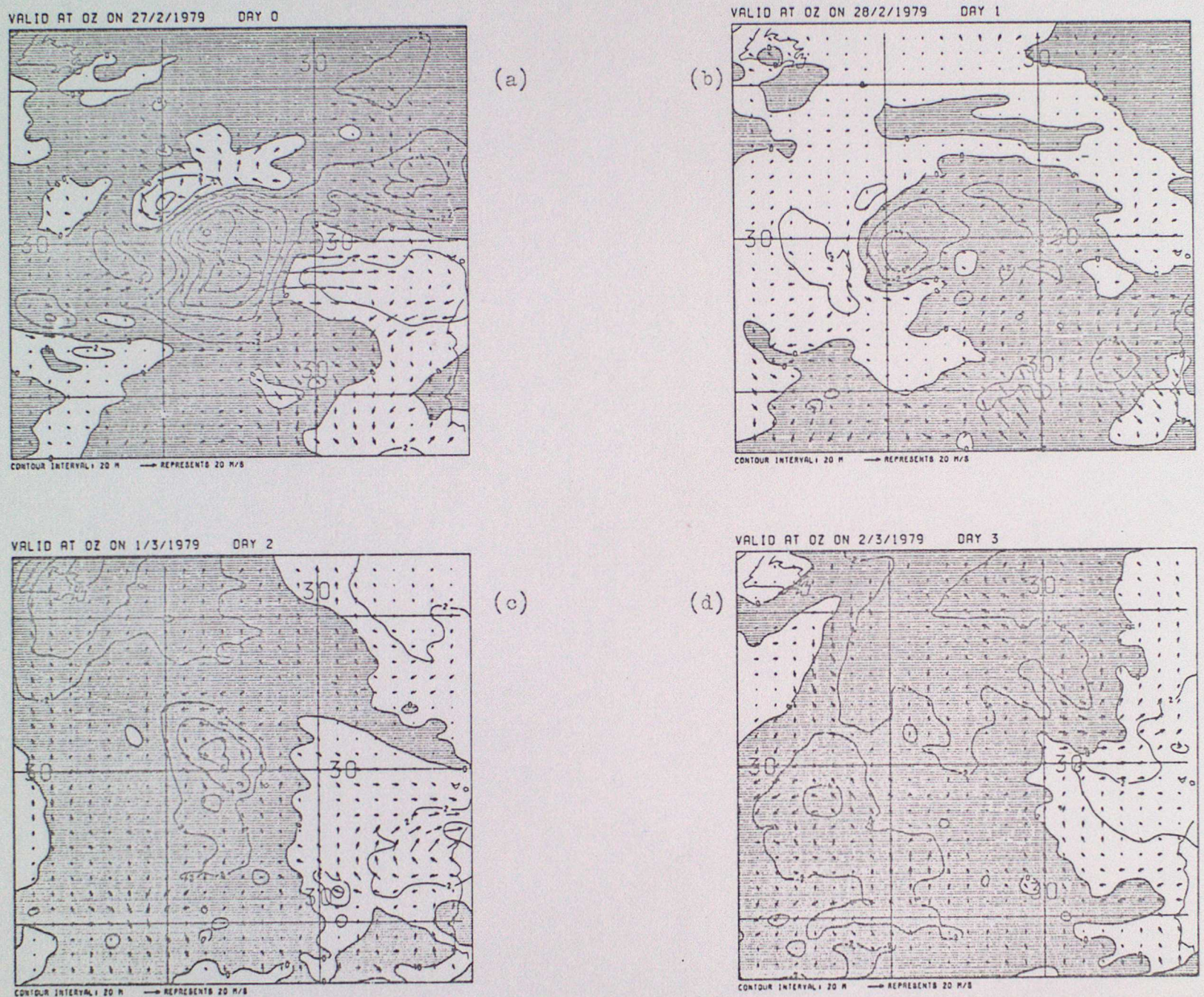

FIGURE 8

Height and Wind Differences at 250mb, N.Atlantic

a) IA3 - IA0, Day 0

b) IA3 - IA1, Day 1

c) IA3 - IA1, Day 2

d) IA3 - IA1, Day 3

a) EXPERIMENT IA0 (CONTROL ASSIMILATION)
NON-DIVERGENT WIND VECTORS & ISOTACHS (M/S) TROPICAL ATLANTIC
VALID AT 0Z ON 27/2/1979
LEVEL: 850 MB

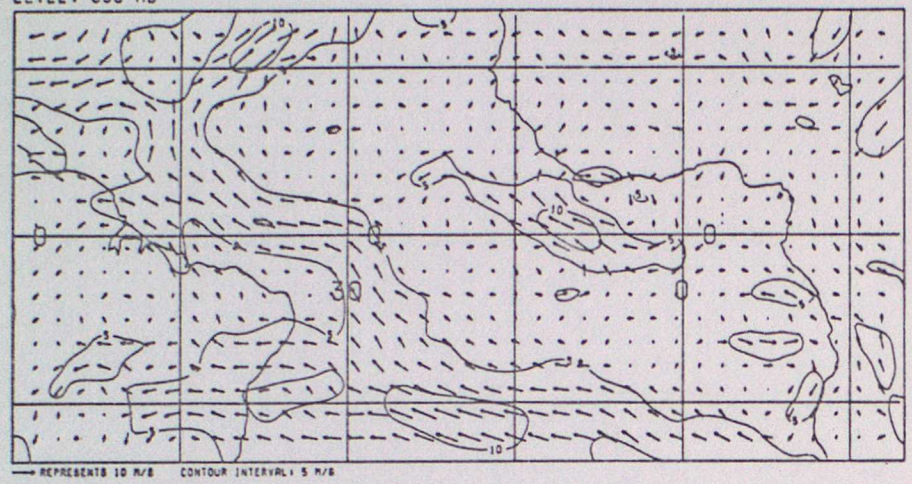

b) EXPERIMENT IA0 (CONTROL ASSIMILATION)
IRROTATIONAL WIND VECTORS & ISOTACHS (M/S) TROPICAL ATLANTIC
VALID AT 0Z ON 27/2/1979
LEVEL: 850 MB

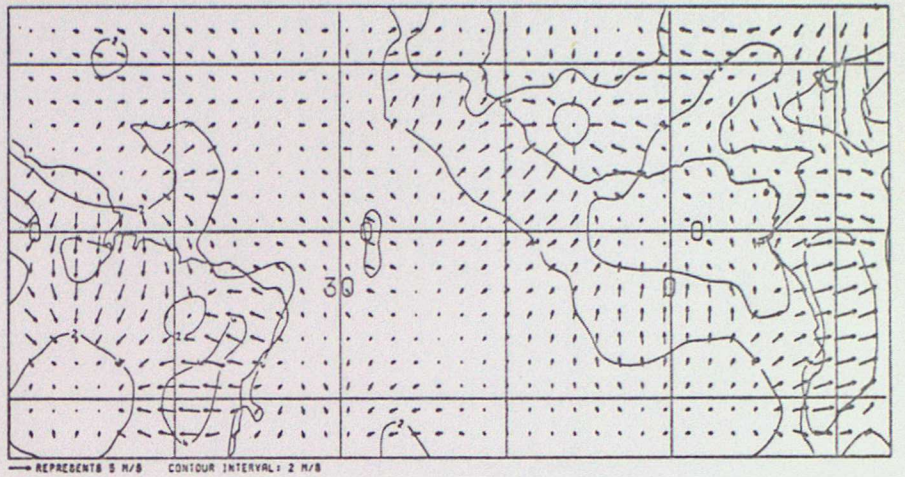

c) EXPERIMENT IA3 (NO SATOBS)
NON-DIVERGENT WIND VECTORS & ISOTACHS (M/S) TROPICAL ATLANTIC
VALID AT 0Z ON 27/2/1979
LEVEL: 850 MB

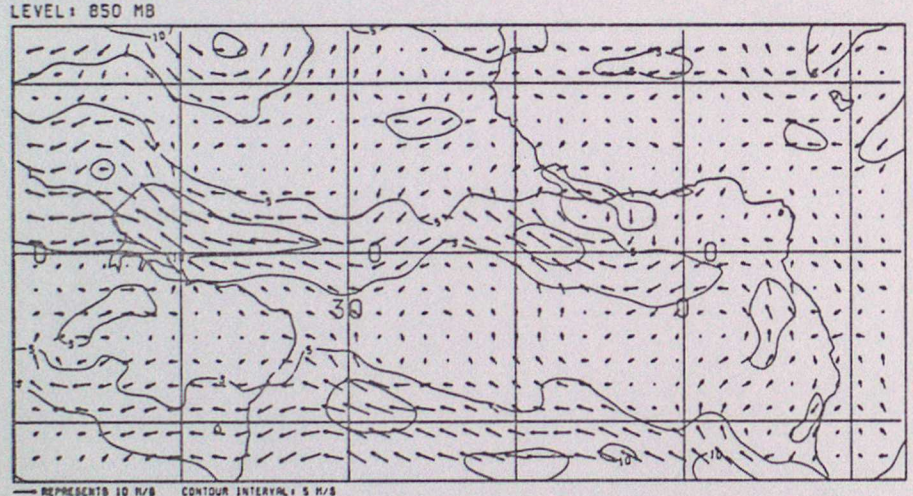

d) EXPERIMENT IA3 (NO SATOBS)
IRROTATIONAL WIND VECTORS & ISOTACHS (M/S) TROPICAL ATLANTIC
VALID AT 0Z ON 27/2/1979
LEVEL: 850 MB

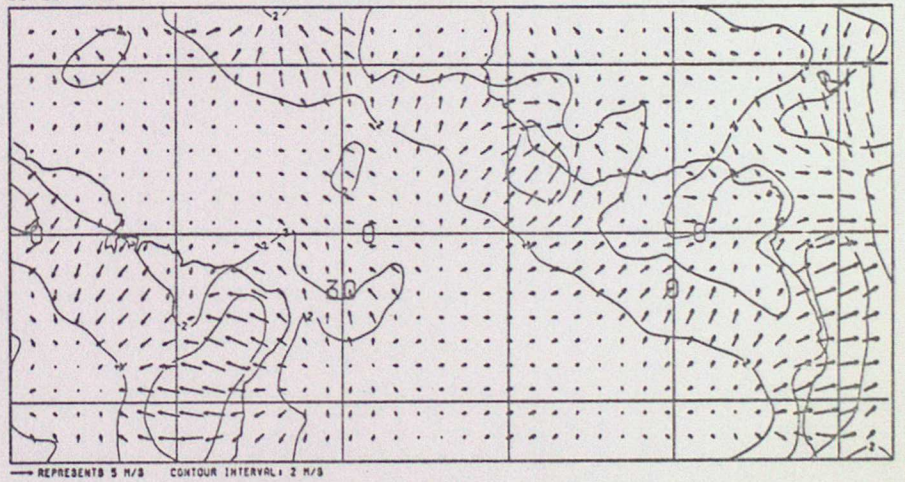

FIGURE 9 Non-Divergent and Irrotational Winds at 850mb over the Tropical Atlantic

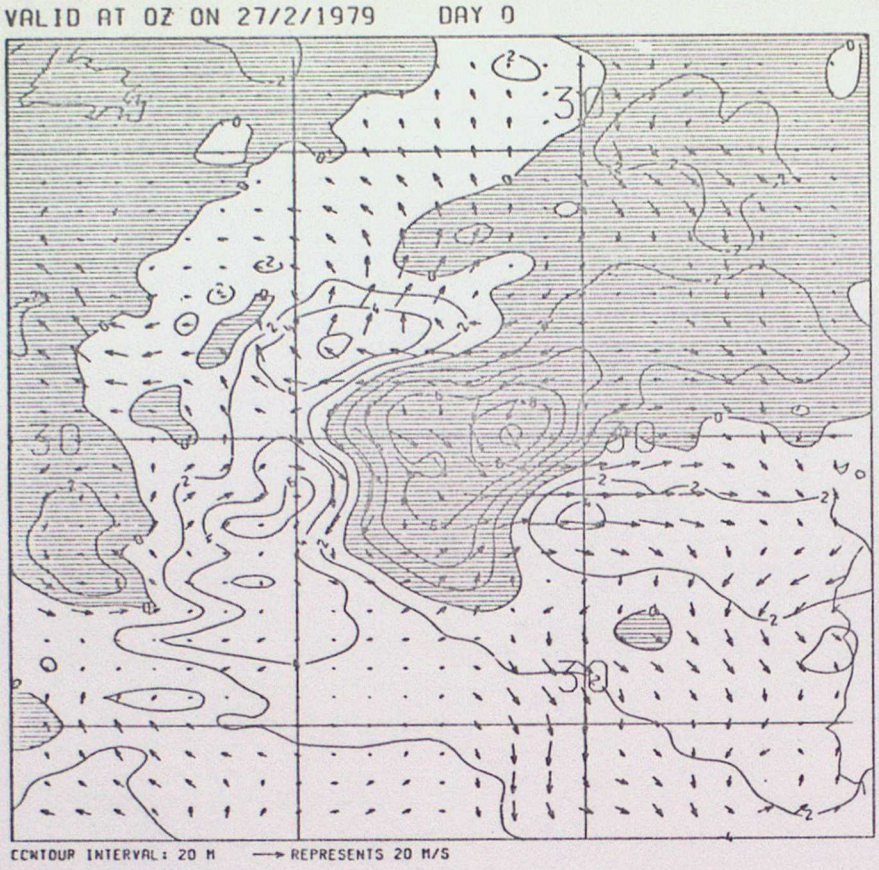

FIGURE 10a

Height and Wind Differences at 250mb, IA4 - IA0, Day 0, North Atlantic

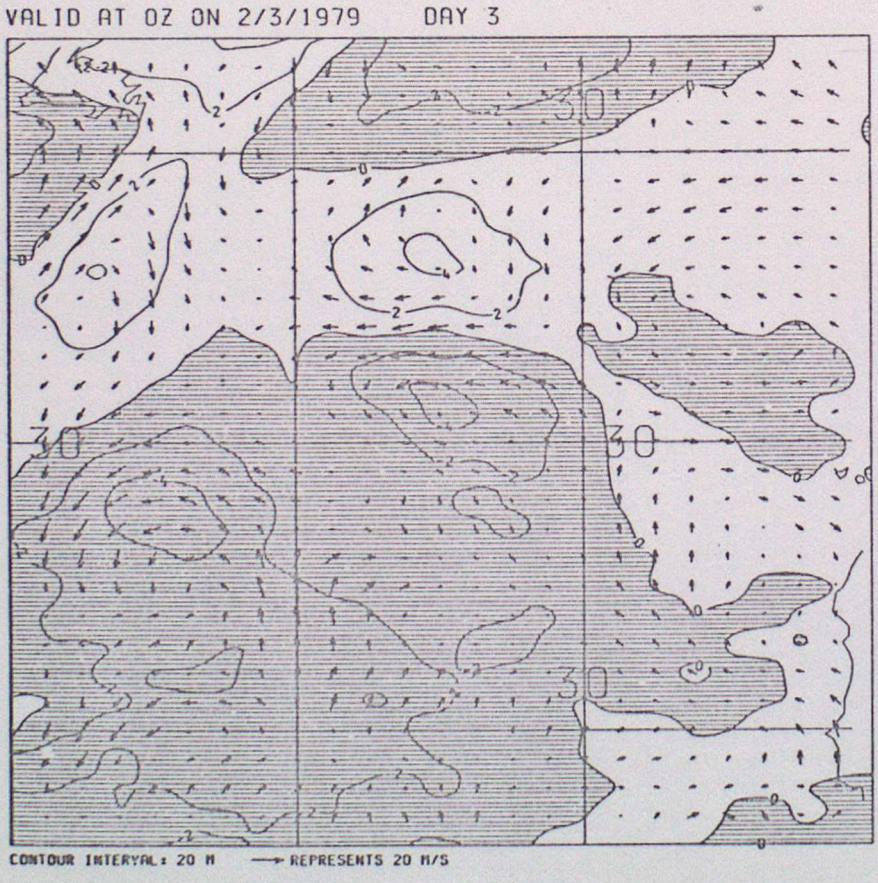

FIGURE 10b

Height and Wind Differences at 250mb, IA4 - IA1, Day 3, North Atlantic

a) VALID AT 0Z ON 27/2/1979 DAY 0

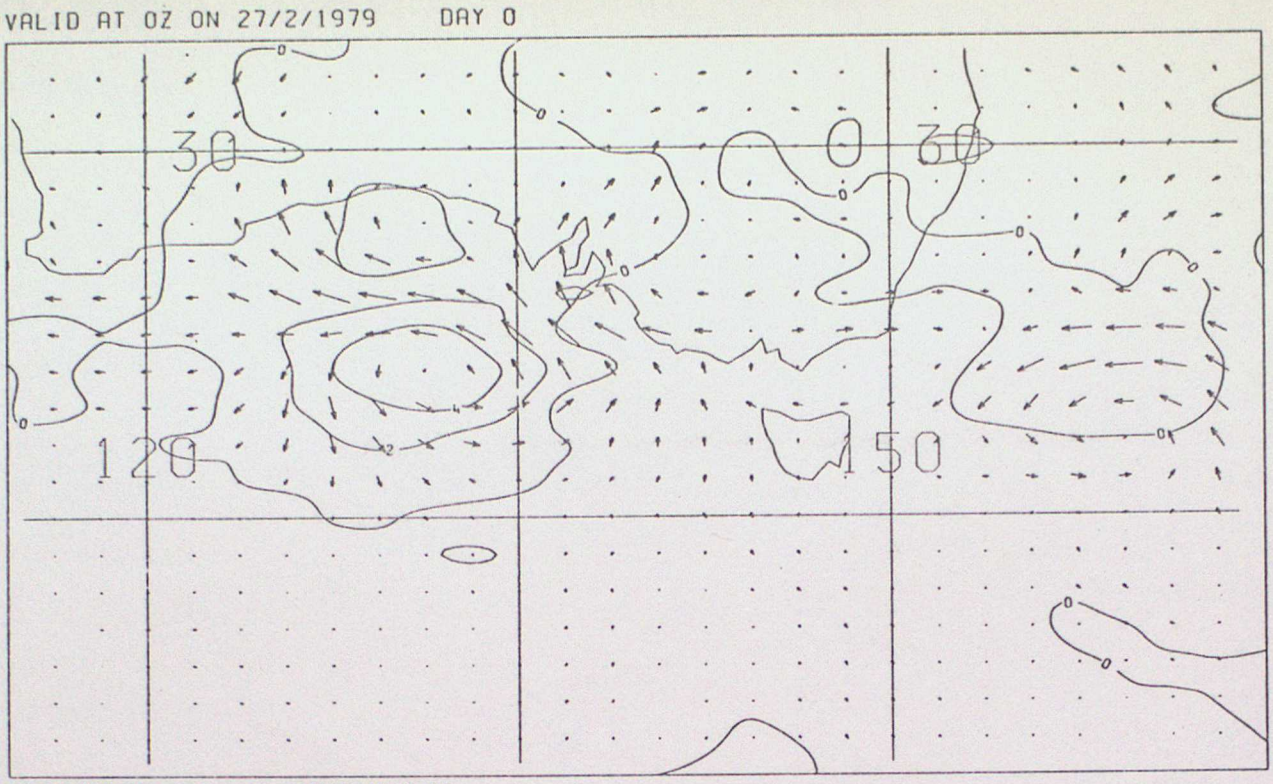

b) VALID AT 12Z ON 27/2/1979 DAY 0

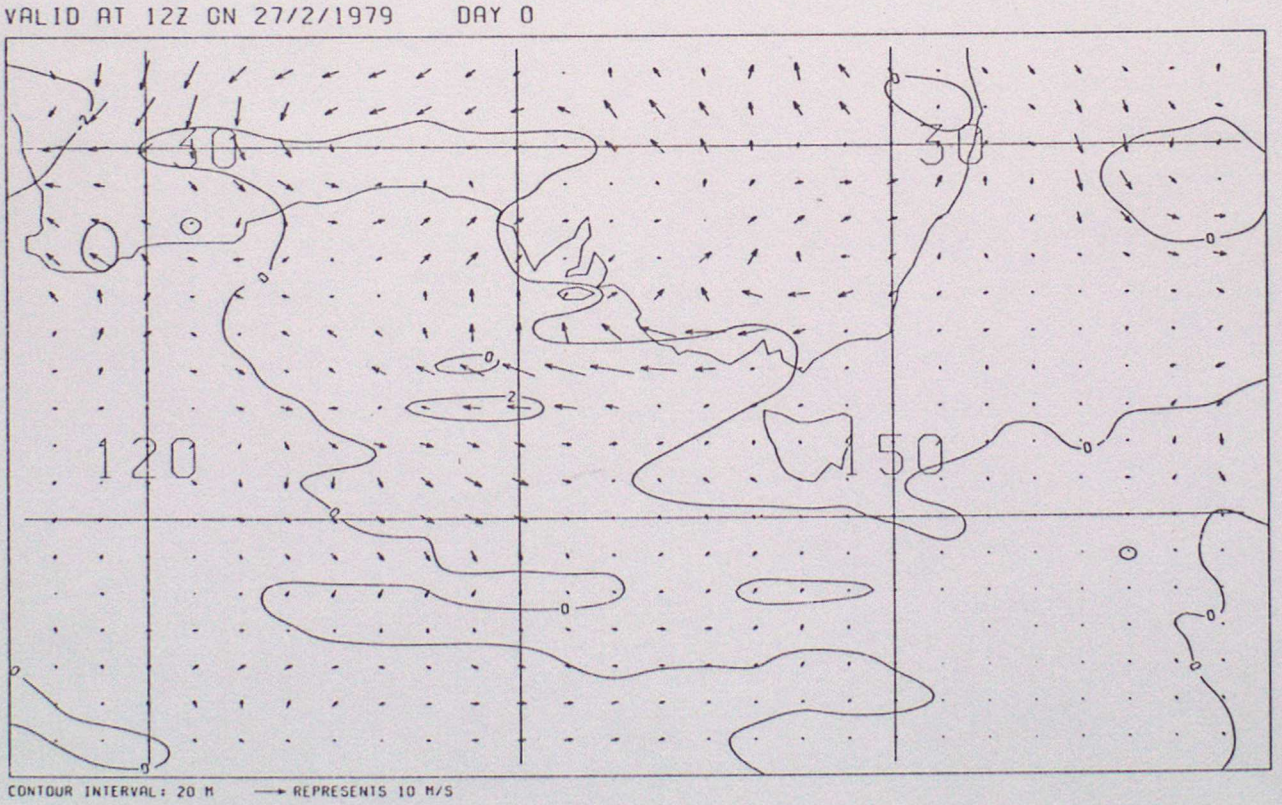

FIGURE 11 Height and Wind Differences at 250mb, Australia:
a) IA5 - IA0, Day 0, Hour 0, b) IA5 - IA1, Day 0, Hour 12

a) VALID AT 0Z ON 27/2/1979 DAY 0

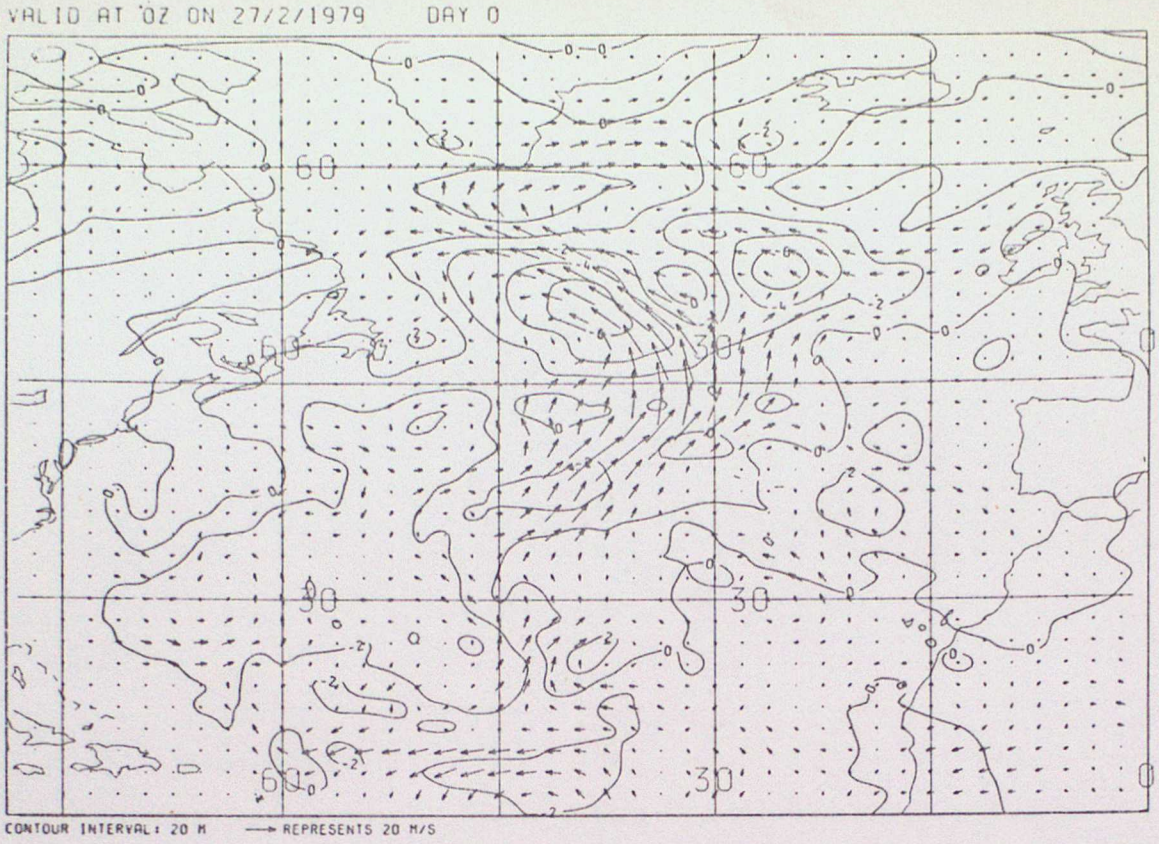

b) VALID AT 12Z ON 27/2/1979 DAY 0

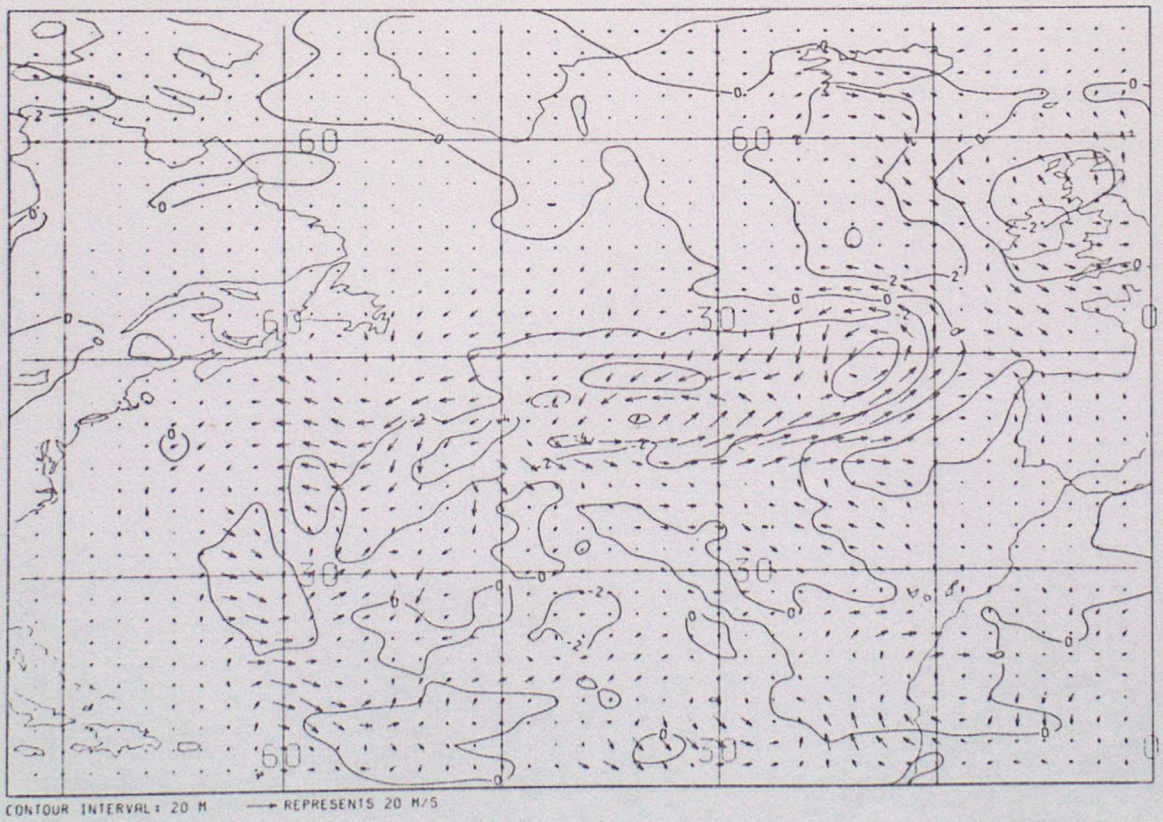

FIGURE 12 Height and Wind Differences at 250mb, North Atlantic:
a) IA5 - IAO, Day 0, Hour 0, b) IA5 - IAO, Day 0, Hour 12

a) GEOPOTENTIAL HEIGHT IA6 (NO DRIFTING BUOYS) - IA0 (CONTROL ASSIMILATION)
VALID AT 0Z ON 27/2/1979 DAY 0
ZONAL RMS DIFFERENCE VALUES > 2.0 SHADED

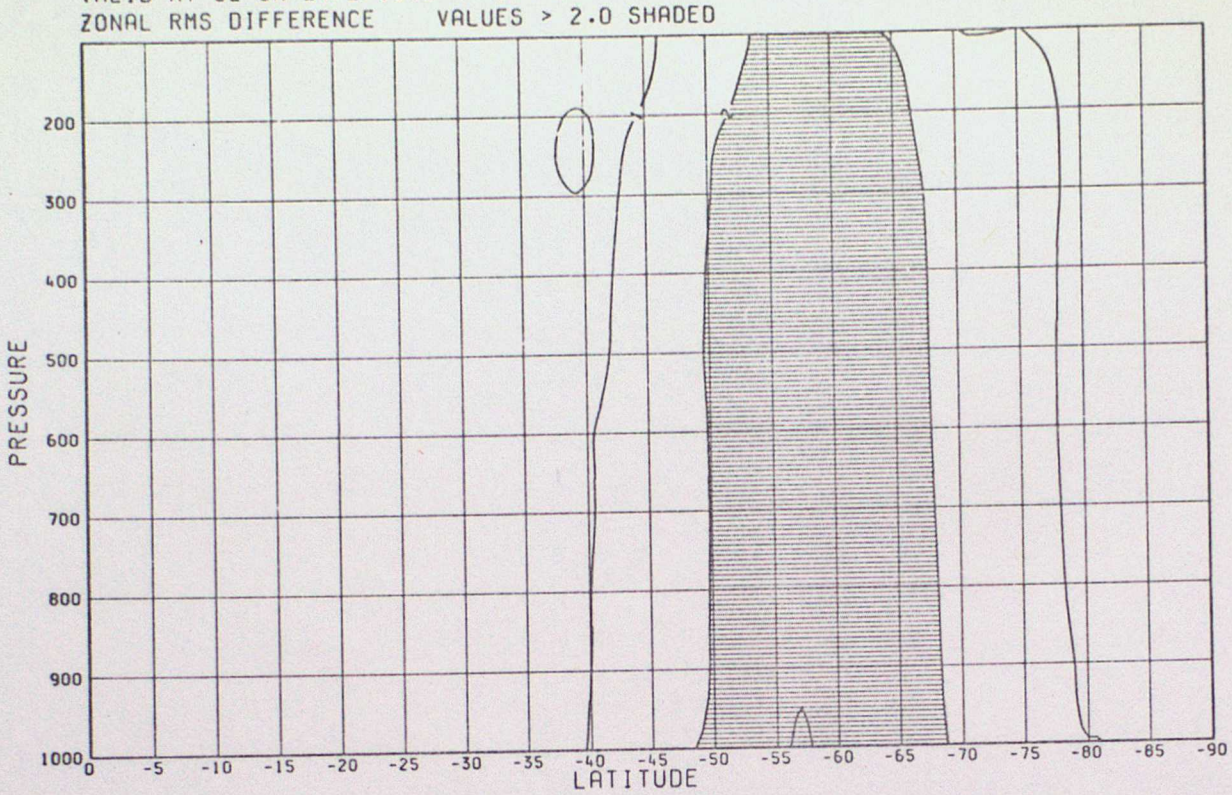

b) GEOPOTENTIAL HEIGHT IA6 (NO DRIFTING BUOYS) - IA1 (CONTROL FORECAST)
VALID AT 0Z ON 2/3/1979 DAY 3
ZONAL RMS DIFFERENCE VALUES > 2.0 SHADED

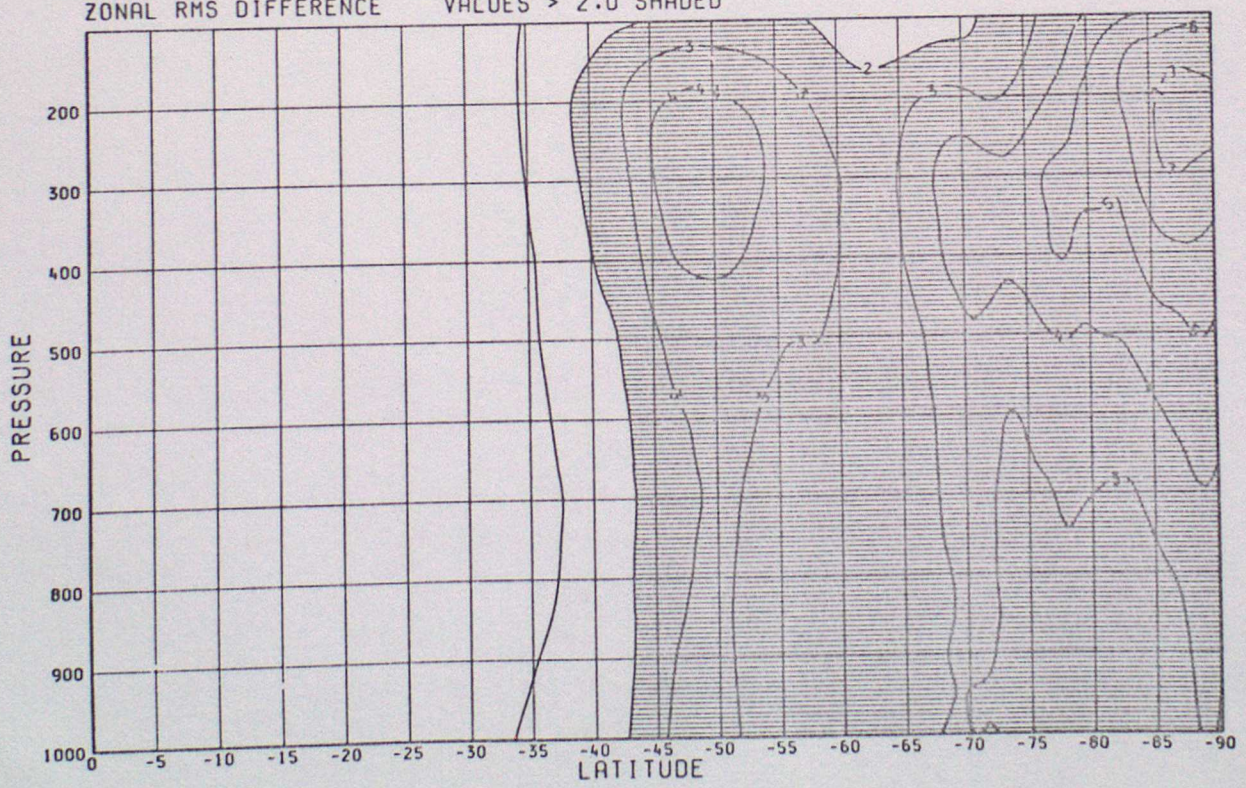

FIGURE 13 Zonal Cross-Sections of rms Height Differences, Impact Study IA6 (no Dribus): a) Day 0, b) Day 3

a) VALID AT 0Z ON 27/2/1979 DAY 0

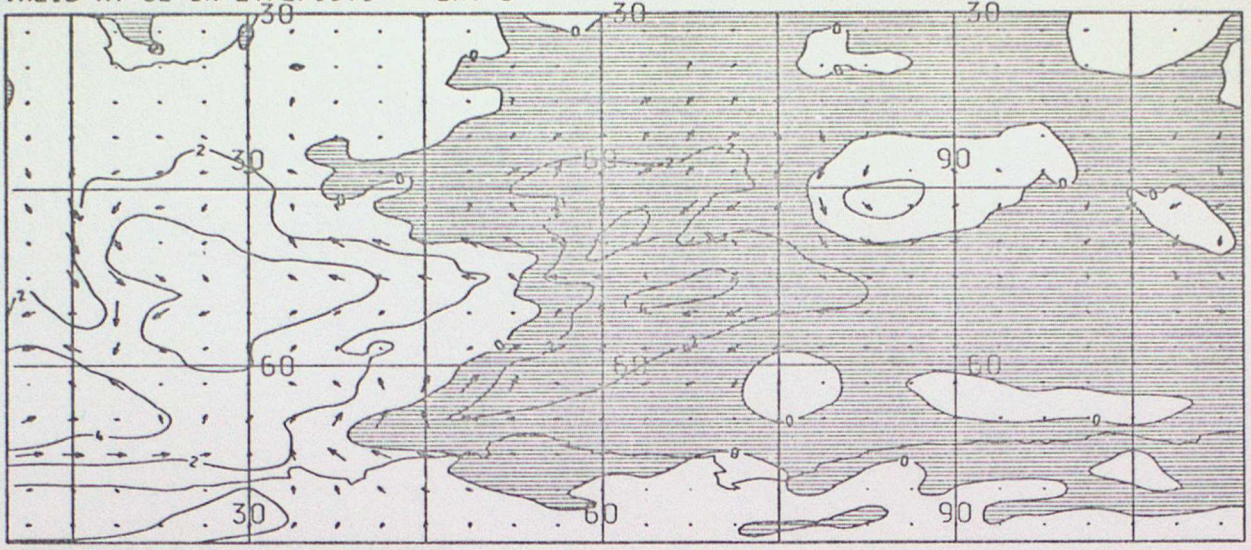

b) VALID AT 0Z ON 2/3/1979 DAY 3

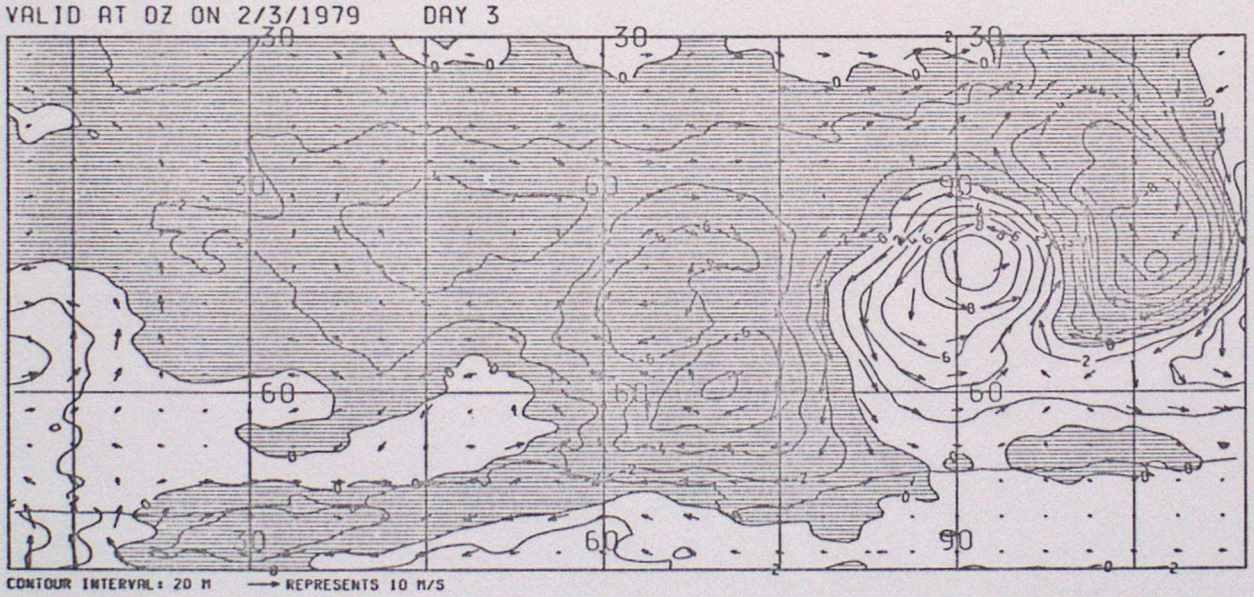

FIGURE 14 Height and Wind Differences at 250mb, Southern Indian Ocean: a) IA6 - IA0, Day 0, b) IA6 - IA1, Day 3

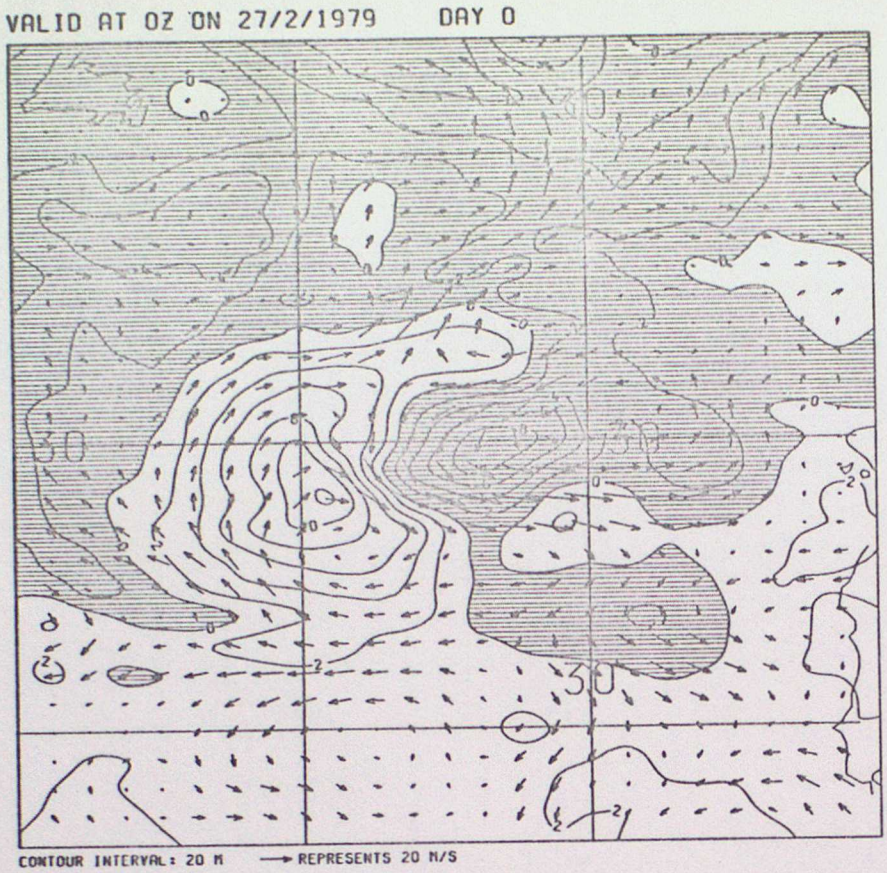

FIGURE 15a

Height and Wind Differences at 250mb, IA7 - IA0, Day 0, North Atlantic

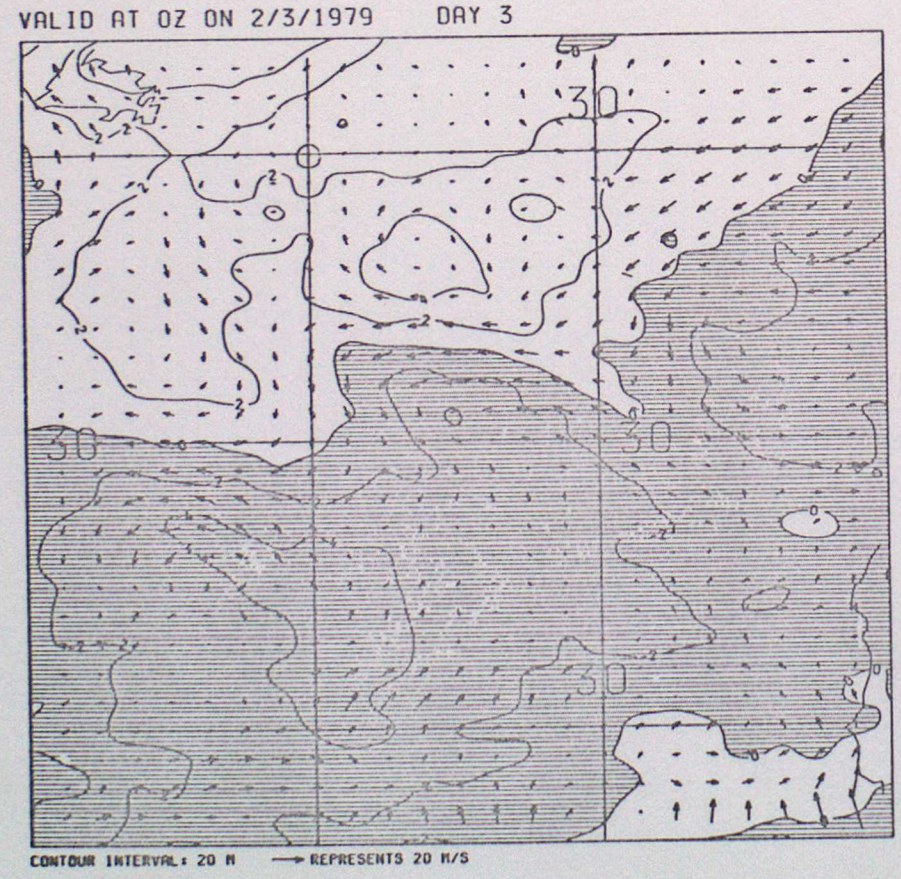

FIGURE 15b

Height and Wind Differences at 250mb, IA7 - IA1, Day 3, North Atlantic

a) VALID AT 0Z ON 27/2/1979 DAY 0

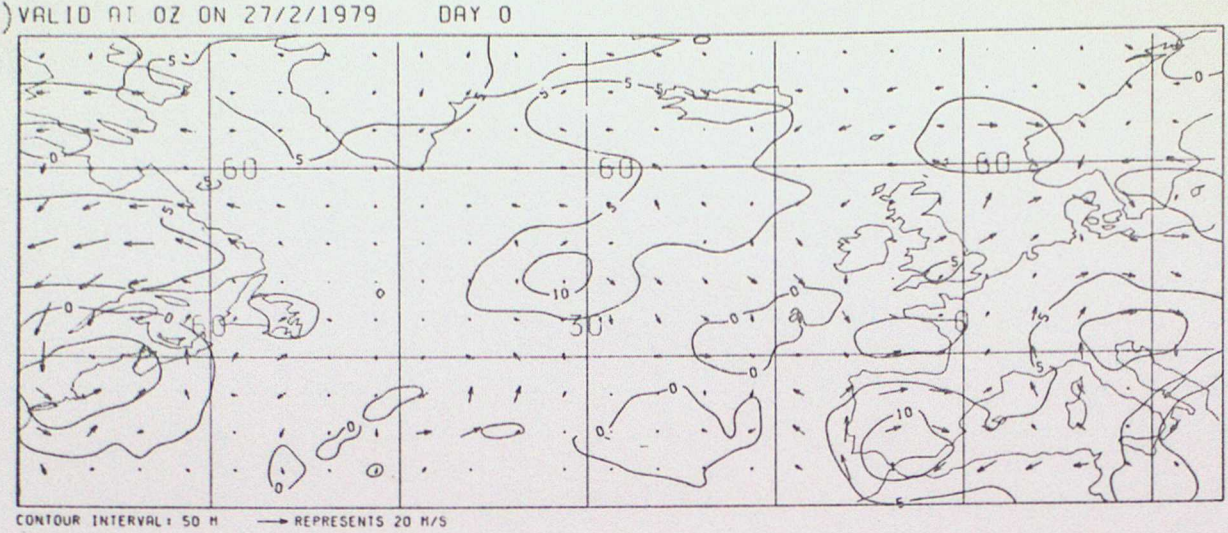

b) VALID AT 0Z ON 2/3/1979 DAY 3

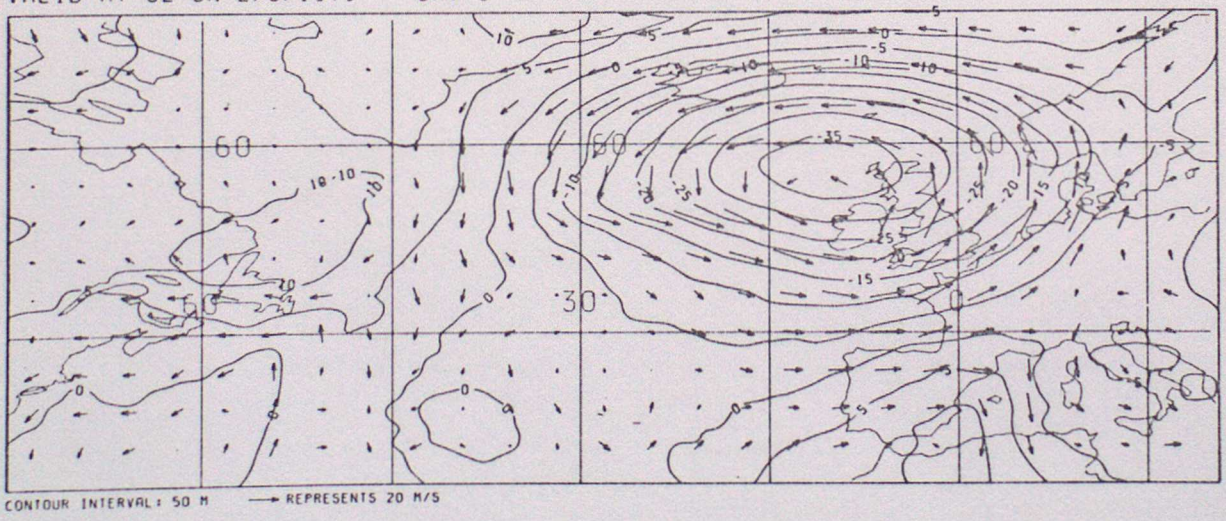

FIGURE 16 Height and Wind Differences at 250mb, North Atlantic: a) IA8 -IA0, Day 0, b) IA8 - IA1, Day 3

FIGURE 17a GLOBAL RMS HEIGHT DIFFERENCES

Expt IA2 (No Satems), Day 3

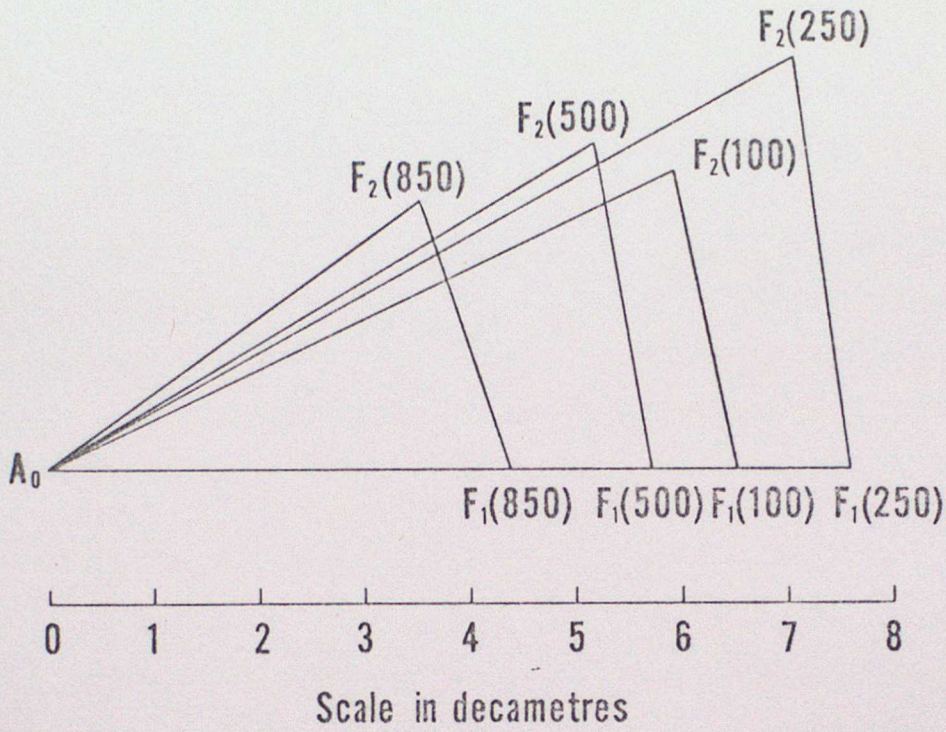

3615

FIGURE 17b REGIONAL RMS HEIGHT DIFFERENCES

Expt IA2 (No Satems) Day 3 250 mb

N=N.Hemi T=Tropics S=S.Hemi

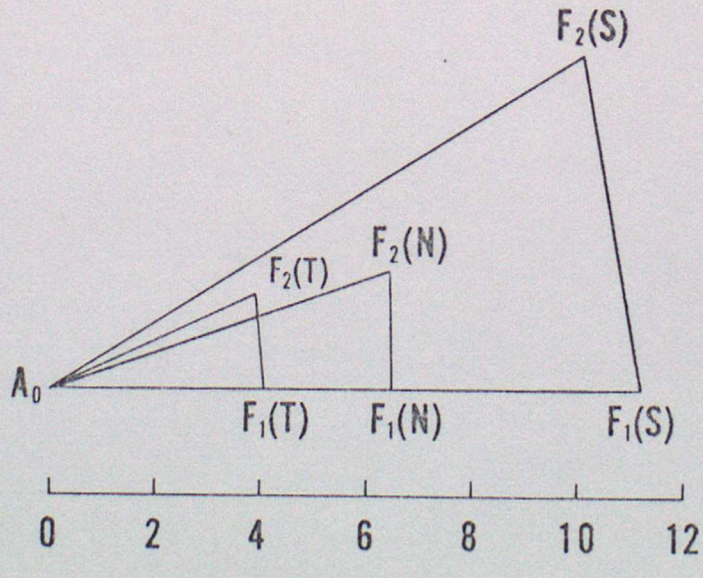

3615